Ornstein

NVO-1253-14

DEVELOPMENT OF A QUASI THREE-DIMENSIONAL GROUNDWATER MODEL FOR A PORTION OF THE NEVADA TEST SITE

By

Phil L. Oberlander

Water Resources Center
Desert Research Institute
University of Nevada System
Reno, Nevada

~~January 1979~~

Prepared for the U.S. Department of Energy, Nevada Operations Office, under contract EY-76-C-08-1253.

HYDROLOGY DOCUMENT NUMBER 204

This report was prepared as an account of work sponsored by the United States Government. Neither the United States nor the United States Energy Research and Development Administration, nor any of their employees, nor any of their contractors, subcontractors, or their employees, makes any warranty, express or implied, or assumes any legal liability or responsibility for the accuracy, completeness or usefulness of any information, apparatus, product or process disclosed, or represents that its use would not infringe privately-owned rights.

AVAILABLE FROM THE NATIONAL TECHNICAL INFORMATION SERVICE

U.S. DEPARTMENT OF COMMERCE

Springfield, VA 22151

Price:	1-50 pps.	$4.00
	51-150 pps.	5.45
	151-325 pps.	7.60

NVO-1253-14

DEVELOPMENT OF A QUASI THREE-DIMENSIONAL GROUNDWATER MODEL FOR A PORTION OF THE NEVADA TEST SITE

By

Phil L. Oberlander

Water Resources Center
Desert Research Institute
University of Nevada System
Reno, Nevada

January 1979

ACKNOWLEDGMENTS

Invaluable assistance from several sources is gratefully acknowledged. For providing the original suggestion as to the nature of this study, the author wishes to thank Dr. Paul R. Fenske. Thanks are also due to Dr. Michael E. Campana for assisting with the computer work.

The author wishes to express deep regret that his original thesis committee chairman, Dr. George B. Maxey, passed away before completion of this project.

CONTENTS

	Page
ABSTRACT	iv
INTRODUCTION	1
FINITE DIFFERENCE EQUATIONS	1
Mathematical Basis for Finite Difference Equations	1
Boundary Conditions for Finite Difference Equations	5
DEVELOPMENT OF A QUASI THREE-DIMENSIONAL CORRECTION MATRIX	7
GEOLOGY AND HYDROGEOLOGY FROM PAHUTE MESA TO YUCCA FLAT, NEVADA TEST SITE	15
Introduction	15
Regional Geologic Setting	19
Rock Units with Associated Values of Hydraulic Conductivities	19
Table 1	20
Structures	31
GROUNDWATER MODEL OF PAHUTE MESA TO YUCCA FLAT	32
CONCLUSIONS	37
BIBLIOGRAPHY	38
APPENDIX A. HEAD VALUES FOR THEORETICAL BASIN	41
Table 2	42
Table 3	43
APPENDIX B. CORRECTION MATRICES	44
Table 4	45
Table 5	46
Table 6	47
APPENDIX C. GROUNDWATER POTENTIAL MODEL	48
Table 7	49
APPENDIX D. COMPUTER MODEL PROGRAMS	51

ABSTRACT

Groundwater systems are often modeled on computers using a finite difference method in two dimensions, height and length. These models do not account for water movement in the lateral extent normal to the model. An empirical correction matrix has been devised that will partially adjust a two-dimensional model for flow in the third dimension. In an isotropic and homogeneous medium, the correction matrix averages a 4.9% difference in potential values.

The correction matrix has been applied to the groundwater system from Pahute Mesa to Yucca Flat on the Nevada Test Site, a distance of 24 kilometers. The geology of the area is complex and contains folded and thrust faulted Paleozoic through Tertiary rocks. Groundwater is recharged at Pahute Mesa and flows to Yucca Flat at the rate of 64.8 acre feet/year. The maximum water flow under all of Yucca Flat and into the Ash Meadows groundwater system is 1240 acre feet year.$^{-1}$.

INTRODUCTION

The purpose of this project is to better define and understand the groundwater system from southern Pahute Mesa to Yucca Flat, Nevada. The area studied lies entirely within the Nevada Test Site, located 90 kilometers north of Las Vegas, Nevada. Because of the radioactive contamination of groundwater at the Nevada Test Site, it is important to understand the regional groundwater movement.

Funding for this project came from the University of Nevada, Desert Research Institute, Water Resources Center as a part of the Groundwater Study Project of the Department of Energy. All computer work was done at the University of Nevada, Reno, on a Control Data Corporation #6400.

FINITE DIFFERENCE EQUATIONS

Mathematical Basis For Finite Difference Equations

Two types of equations are useful in groundwater modeling problems. First are continuity equations that express the conservation of mass. Second are momentum equations, such as Darcy's Law, that define flow through a saturated isotropic porous medium. These two types of equations are combined to yield a groundwater flow equation that is applicable to the region studied (Huntoon, 1972).

The following is developed in the two dimensions Y, Z.

GIVEN: Continuity equation for fluid in a porous medium.

$$-\frac{\partial(\rho V_y)}{\partial y} - \frac{\partial(\rho V_z)}{\partial z} = \frac{\partial \rho}{\partial t} \qquad \text{Eq. 1}$$

Where ρ = density of fluid (ML^{-3})

t = time

V_z = specific discharge in Z direction (LT^{-1})

V_y = specific discharge in Y direction (LT^{-1})

AND: Darcy's Law for flow through a porous medium (empirical).

$$V_s = -K \frac{\partial \phi}{\partial s} . \qquad \text{Eq. 2}$$

Where V_s = specific discharge in the s direction (LT^{-1})

K = hydraulic conductivity of isotropic medium (LT^{-1})

ϕ = hydraulic head (L)

s = direction of flow (L)

Under isotropic conditions, Darcy's Law can be written in vector components

$$V_y = -K\frac{\partial \phi}{\partial y} \qquad V_z = -K\frac{\partial \phi}{\partial z}. \qquad \text{Eq. 3}$$

Substituting the vector components of Darcy's Law into the equation of continuity yields

$$\frac{\partial (\rho K\frac{\partial \phi}{\partial y})}{\partial y} + \frac{(\rho K\frac{\partial \phi}{\partial z})}{\partial z} = \frac{\partial \rho}{\partial t} \qquad \text{Eq. 4}$$

Which is the equation governing a compressible fluid in an isotropic, heterogeneous porous medium. If we assume that the density is constant, the hydraulic conductivity is constant and steady state conditions prevail, then Eq. 4 reduces to

$$\frac{\partial^2 \phi}{\partial y^2} + \frac{\partial^2 \phi}{\partial z^2} = 0 \qquad \text{Eq. 5}$$

This is the Laplace Equation for groundwater flow and is quite difficult to integrate except for the simplest boundary condition.

To find the finite difference equation for an interior node, the second order partial derivatives of Laplace's Equation must be replaced. For any value of (Y,Z) the equation for ϕ (Y,Z) can be expanded about any point (Y_O,Z_O) (Boas, 1966).

$$\phi(Y,Z) = \phi(Y_0,Z_0) + \frac{\partial}{\partial y}\phi(Y_0,Z_0)(Y-Y_0) + \frac{\partial}{\partial z}\phi(Y_0,Z_0)(Z-Z_0)$$

$$+ \frac{1}{2!}\left[\frac{\partial^2}{\partial y^2}\phi(Y_0,Z_0)(Y-Y_0)^2 + 2\frac{\partial^2}{\partial y \partial z}\phi(Y_0,Z_0)(Y-Y_0)(Z-Z_0)\right.$$

$$\left. + \frac{\partial^2}{\partial z^2}\phi(Y_0,Z_0)(Z-Z_0)^2\right] + Rn \qquad \text{Eq. 6}$$

Where Y = next node in the positive direction on the Y axis

Y_O = any Y

Z = next node in the positive direction on the Z axis

Z_O = any Z

(Y_O,Z_O) = point about which the series expansion is taken

Rn = a small remainder representing the other terms in the series

See figure 1.

By use of a forward and a backward difference technique (Freeze, 1969, p. 45), which is too extensive to present here, the second order derivatives of the Laplace Equation are approximated by

$$\frac{\partial^2\phi}{\partial y^2} \approx \frac{\phi_3 + \phi_4 - 2\phi_0}{R^2} \qquad \text{Eq. 7}$$

and

$$\frac{\partial^2\phi}{\partial z^2} \approx \frac{\phi_1 + \phi_2 - 2\phi_0}{R^2}. \qquad \text{Eq. 8}$$

By substituting values for the derivatives in Eq. 5 and letting R equal one nodal space, the equation becomes

Figure 1

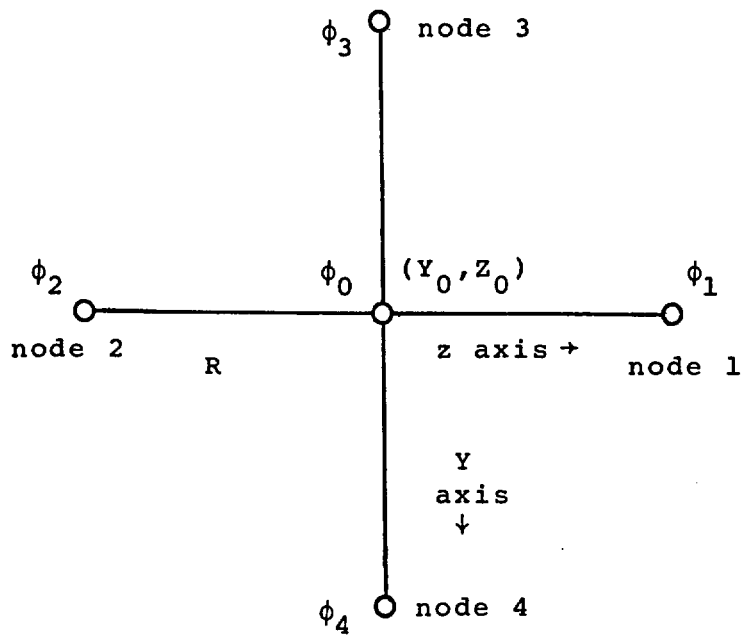

Where

node 1 = the first node along the forward distance along the Z axis used in Eq. 6

node 2 = the first node along the backward distance along the Z axis used in Eq. 6

node 3 = the first node along the forward distance along the Y axis used in Eq. 6

node 4 = the first node along the backward distance along the Y axis used in Eq. 6

R = the nodal spacing in both the Y and Z directions

$$\sum_{1}^{N=4} \phi_N - 4\phi_0 = 0 \qquad \text{Eq. 9}$$

which is the finite difference approximation of Laplace's Equation for any constant R. By algebra,

$$\frac{1}{4}\sum_{1}^{N=4} \phi_N = \phi_0 \qquad \text{Eq. 10}$$

for any interior node in an isotropic, homogeneous medium. Or, by other notations, Eq. 10 becomes

$$\phi(Y,Z)^{i+1} = \tfrac{1}{4}(\phi(Y+1,Z)^{i} + \phi(Y-1,Z)^{i} + \phi(Y,Z+1)^{i} + \phi(Y,Z-1)^{i}). \qquad \text{Eq. 11}$$

Where (Y,Z) = the node where head is to be determined

i = the number of iteration

Eq. 11 is known as the Jacobi Method and is theoretically important. However, other techniques are better suited to computer means of matrix relaxation. This paper uses the Gauss-Seidel Method exclusively, which is about twice as fast in machine time as the Jacobi Equation. In the Gauss-Seidel Method the heads at nodes (Y-1,Z) and (Y,Z-1) have already been computed by iteration i+1 when node (Y,Z) is computed. The Gauss-Seidel Method is

$$\phi(Y,Z)^{i+1} = \tfrac{1}{4}(\phi(Y+1,Z)^{i} + \phi(Y-1,Z)^{i+1} + \phi(Y,Z+1)^{i} + \phi(Y,Z-1)^{i+1}) \qquad \text{Eq. 12}$$

Boundary Conditions for Finite Difference Equations

Along the water table, $\phi = h$, where h = the distance above the datum - usually mean sea level. At depth there is an assumed impermeable basement where $\partial\phi/\partial y = 0$ and $\partial\phi/\partial z$ 0, which is a zero flux condition. In order to position a zero flux condition in the Y direction (at the basement) at node (Y,Z), let $\phi(Y+1,Z) = \phi(Y,Z)$. The same procedure is used to place an impermeable boundary along the sides of the matrix in order to model a closed system. The equation becomes $\phi(Y,Z+1) = \phi(Y,Z)$ in the positive Z direction. The location of the boundary is halfway between Z and Z+1. Where the impermeable basement, zero flux in the Y direction, meets the side of the matrix, zero flux in the Z direction, a special boundary condition exists. The conditions are met in the corners of the matrix and the equation $\phi(Y+1,Z+1) = \phi(Y,Z)$ applies. The location of this boundary is halfway between Z and Z+1, and is also halfway between Y and Y+1.

In an isotropic heterogeneous medium, different hydraulic conductivities are used within the matrix to model different rock types. When using computer models to solve for the head potentials, the absolute values of hydraulic conductivity are not needed as long as the ratios between the values are known. This does not apply to time-dependent situations. Within any layer where K does not change, the Gauss-Seidel Model applies. The boundary between two different hydraulic conductivities is modeled in this paper by a harmonic mean technique which places the boundary between two hydraulic conductivities, K_1 and K_2, between nodes (Y,Z) and (Y+1,Z) (Huntoon, 1972) (see Figure 2).

```
              Z axis  →

(Y-1,Z-1)  (Y-1,Z)  (Y-1,Z+1)
    O         O         O

(Y,Z-1)    (Y,Z)    (Y,Z+1)          Y axis
   O         O        O                 ↓
                                      K1
-------------------------------------------
                                      K2

(Y+1,Z-1)  (Y+1,Z)  (Y+1,Z+1)
    O         O         O

(Y+2,Z-1)  (Y+2,Z)  (Y+2,Z+1)
    O         O         O
```

Figure 2

To compute the head at (Y,Z) and (Y+1,Z) the harmonic mean equations are respectively:

$$\phi(Y,Z) = (K_1(Y,Z-1)\phi(Y,Z-1)+K_1(Y,Z+1)\phi(Y,Z+1)+ K_1(Y-1,Z)\phi(Y-1,Z)+K_{har}\phi(Y+1,Z)) \; / \; (K_1(Y,Z-1)+K_1(Y,Z+1)+K_1(Y-1,Z)+K_{har}$$

and

$$\phi(Y+1,Z) = (K_2(Y+1,Z-1)\phi(Y+1,Z-1)+ K_2(Y+1,Z+1)\phi(Y+1,Z+1)+K_2(Y+2,Z)\phi(Y+2,Z)+K_{har} \phi(Y,Z)) \,/(K_2(Y+1,Z-1)+K_2(Y+1,Z+1)+ K_2(Y+2,Z)+K_{har})$$

Where $K_1(Y,Z)$ = hydraulic conductivity number 1 at point (Y,Z)

$K_2(Y+1,Z)$ = hydraulic conductivity number 2 at point (Y+1,Z)

K_{har} = Harmonic mean hydraulic conductivity which equals

$$\frac{(2K_1)\ (K_2)}{K_1 + K_2}.$$

DEVELOPMENT OF A QUASI THREE-DIMENSIONAL CORRECTION MATRIX

The implementation of finite difference equations is best suited to computer programs using recursive procedures. Finite difference equations are used with recursive procedures to allow the computer solution to converge on the exact solution, represented by the partial differential equation. The difference between the exact solution and the computer solution (convergence criteria) is ± 0.000001 in this paper. All recursive programs have been converged to the same tolerances.

Although groundwater hydraulics are three-dimensional, they are usually solved by two-dimensional finite difference equations. This is done for several reasons. First, the amount of computer memory needed to solve a three-dimensional problem is much larger than for a two-dimensional problem, although this is less of a problem today than when computers were first used to solve finite difference equations in the 1960's.

R.A. Freeze stated, ". . . at the present time (1966), the use of three-dimensional mathematical models should be limited to small, simple basins that can be adequately represented by 7500 nodes. The best way to handle large, complex basins is with a series of two-dimensional models representing vertical sections taken parallel to the direction of dip to the water table slope" (Freeze, 1969). Today (1978) computer memory capable of 50,000 nodes is commonplace and will cover most modeling situations.

The second reason involves computer time. As the number of nodes increases, the number of computations for a three-dimensional model increases exponentially over the number of steps in a simpler two-dimensional model. It can be seen in Figure 3 that the extra dimension increases the number of computations at a rapid rate.

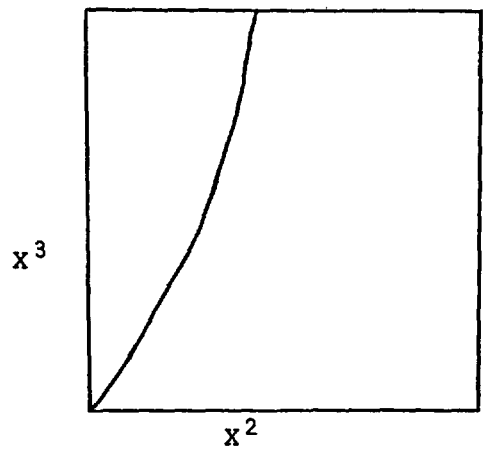

Where X = number of nodes along a unit axis.

Figure 3

The machine time needed to compute the extra dimension can turn computer time into a major expense.

Third, the number and complexity of the finite difference equations increases significantly when a three-dimensional solution is used. The three-dimensional two-layered model used in this paper requires a 350 percent increase in program length over a two-dimensional two-layered model.

For the reasons noted above, the users of two-dimensional models define the basin to be modeled as infinite in the lateral extent. In most cases this assumption allows a simple and fast model that gives acceptable results. However, the assumption carries with it the supposition that the flow paths of the groundwater are parallel in the lateral extent. Under these conditions, areas of recharge or discharge cannot be accurately represented.

The major advantage of three-dimensional models, besides the added geological input, is that they allow water to diverge from a recharge area and to converge at a discharge area. This gives the best possible solution to hydraulic groundwater problems. But how much error is introduced by the use of a two-dimensional model that does not account for water movement in a lateral direction, and can this be partially corrected? To examine this problem, a computer program was written to emperically compare the results of a three-dimensional and a two-dimensional model.

An imaginary basin was envisioned, with a single recharge area and a single discharge area. The water table was linear between the two areas. The values of head chosen for the high and low areas were arbitrarily set at 20 and 10, respectively; steady state conditions were assumed. The aquifer was assumed to be isotropic and the coding allowed for both homogeneous and heterogeneous cases. The development behind the computer program was first aimed at presenting the most basic case possible, with variations of hydraulic conductivity to be added later.

The imaginary basin was modeled by a three-dimensional model called Box and a two-dimensional model known as Mat. Both models were designed so that two different hydraulic conductivities could be examined, an upper horizontal layer of rows Y = 1 to 6.5, and a lower horizontal layer of rows Y = 6.5 to 12. The model Box (see Figure 4) is a (12,21,20) matrix consisting of 5040 nodes. The model Mat (see Figure 5) is a (12,20) matrix having 240 notes. In Figure 6 the space relationship between Box and Mat can be seen. The shaded area is the matrix Mat, centered along the X axis inside the matrix Box. The given water table is initialized along line R-D.

The same criteria was used in both models for depth and length of basin, position and value of the water table, and hydraulic conductivity. Since all parameters are the same, except that the model Box also computes head along the X axis, it can be concluded that any difference in the results are due to water movement in the X direction. This water movement is the expansion of water moving away from the recharge area and the contraction of water approaching the discharge area. The flowline divergence and convergence along the flow paths at the water table is shown by the dotted lines in Figure 6. Homogeneous conditions were assumed and both matrices were relaxed by computer. The results of Mat and the area of Box that corresponds to Mat (see Figure 6) were compared. Both matrices have the same mean value of 15.0.

The range of the computed values is greater in the two-dimensional solution (see Appendix A, Tables 2 and 3). Head values in the recharge area of Mat are too large because there is no divergence of flow in the X direction. Similarly, in the discharge area of Mat there is no convergence of flow in the X direction and the head values are too small. Since the center of the two-dimensional solution lies midway between values that are too large and those that are too small, it is the most accurate

MATRIX BOX

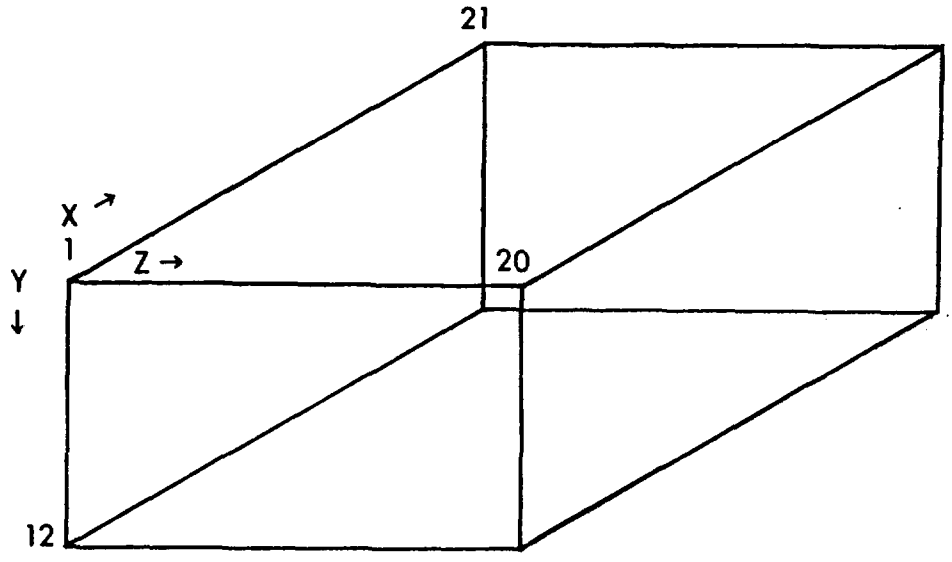

Figure 4

MATRIX MAT

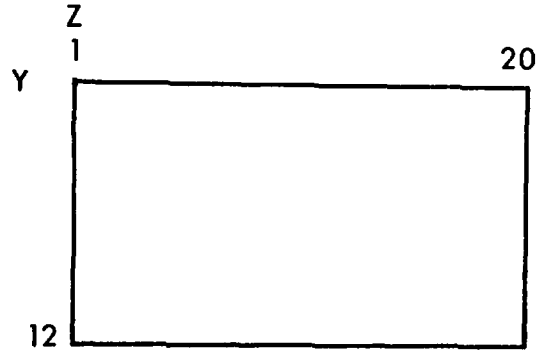

Figure 5

(see Appendix B, Table 4). The water table values have a correction factor of zero because the water table is the same in both models. The zero values are excluded from all statistical analysis of the matrix.

In order to observe and correct for the differences between the two solutions, a new matrix called Corrmat (for correction matrix) was devised. Both the three-

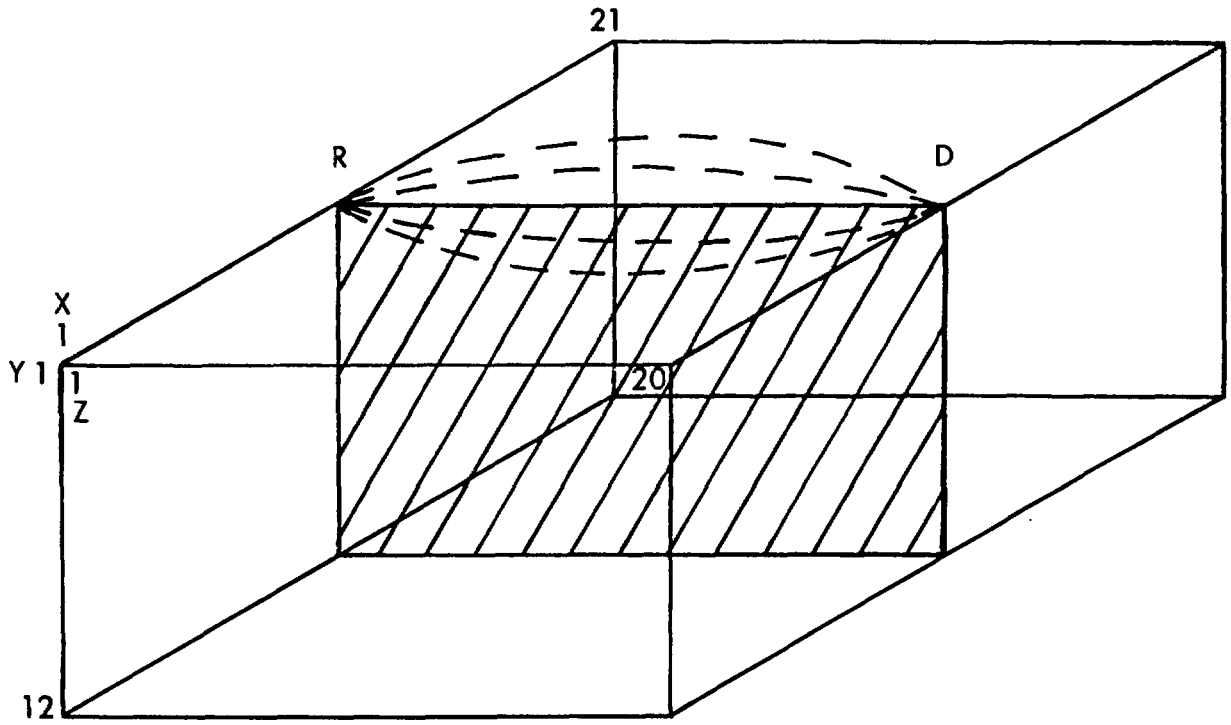

Figure 6 Spacial Relationship of Box and Mat

dimensional and two-dimensional solutions were divided by their mean value of 15.0. This presents each solution as a field of percentages about the mean. Since the values of head in the two-dimensional solution had a greater range, the percentiles also had a greater range. Then, by simply subtracting the percentiles at each node of Mat from the corresponding node of Box, one produces a matrix (12,20) that shows the degree of difference at each point. The Corrmat matrix can be used to correct for flow in the X direction when applied to a two-dimensional solution of a three-dimensional system. To use this correction method:

1. Relax the matrix to be corrected by finite difference means;
2. Either expand or contract the correction matrix by linear methods along the Y and Z axis to fit the matrix to be corrected;
3. Multiply the value at each node in the correction matrix by the mean value of head within the matrix to be corrected;
4. Add the values from step 1 to each corresponding node or group of nodes in matrix to be corrected.

To examine the nature of the correction factor, two different example matrices were computed. A "normal" case of isotropic homogeneous conditions were also computed to see the effect in the ideal case (see Appendix B, Table 4). Two heterogeneous cases are also presented: first, a confined situation with an upper hydraulic conductivity of 1.0 and a lower hydraulic conductivity of 100.0 (see Appendix B, Table 5); second, an unconfined situation of an upper hydraulic conductivity of 100.0 and a lower hydraulic conductivity of 1.0 (see Appendix B, Table 6).

The correction factor is best studied in graphic form. The data from Table 4 are contoured in Figure 7. Isotropic and homogeneous conditions are represented. Observation of Figure 7 shows that the largest amount of correction occurs in the upper portions along the vertical sides. The reason for this is twofold. First, the majority of flow in an isotropic homogeneous groundwater model is near the water table due to the high gradient. Second, the divergence in the X direction is greatest at the recharge-discharge points. Hence the figure can be considered a map of flow potential in the X direction. The correction is zero in the center because the flow is parallel for all flow paths along the vertical normal to the central flow path. The average absolute value of the correction matrix is 4.903%; the largest amount of correction at any node is 10.160%; the standard deviation is 0.0557; and the Kurtosis equals 1.7189.

A two-layered model produces some interesting changes in the correction matrix. The unconfined case is represented by a model with a lower hydraulic conductivity of 1.0 and an upper hydraulic conductivity of two orders of magnitude greater, or 100.00. Figure 8 contours the data in Appendix B, Table 5. The amount of correction is greatest in the upper portions of the matrix and along the ends of the matrix. The unconfined conditions induced a greater amount of flow in the X direction. This is reasonable since one would expect that the water would spread out in the X direction

HOMOGENEOUS

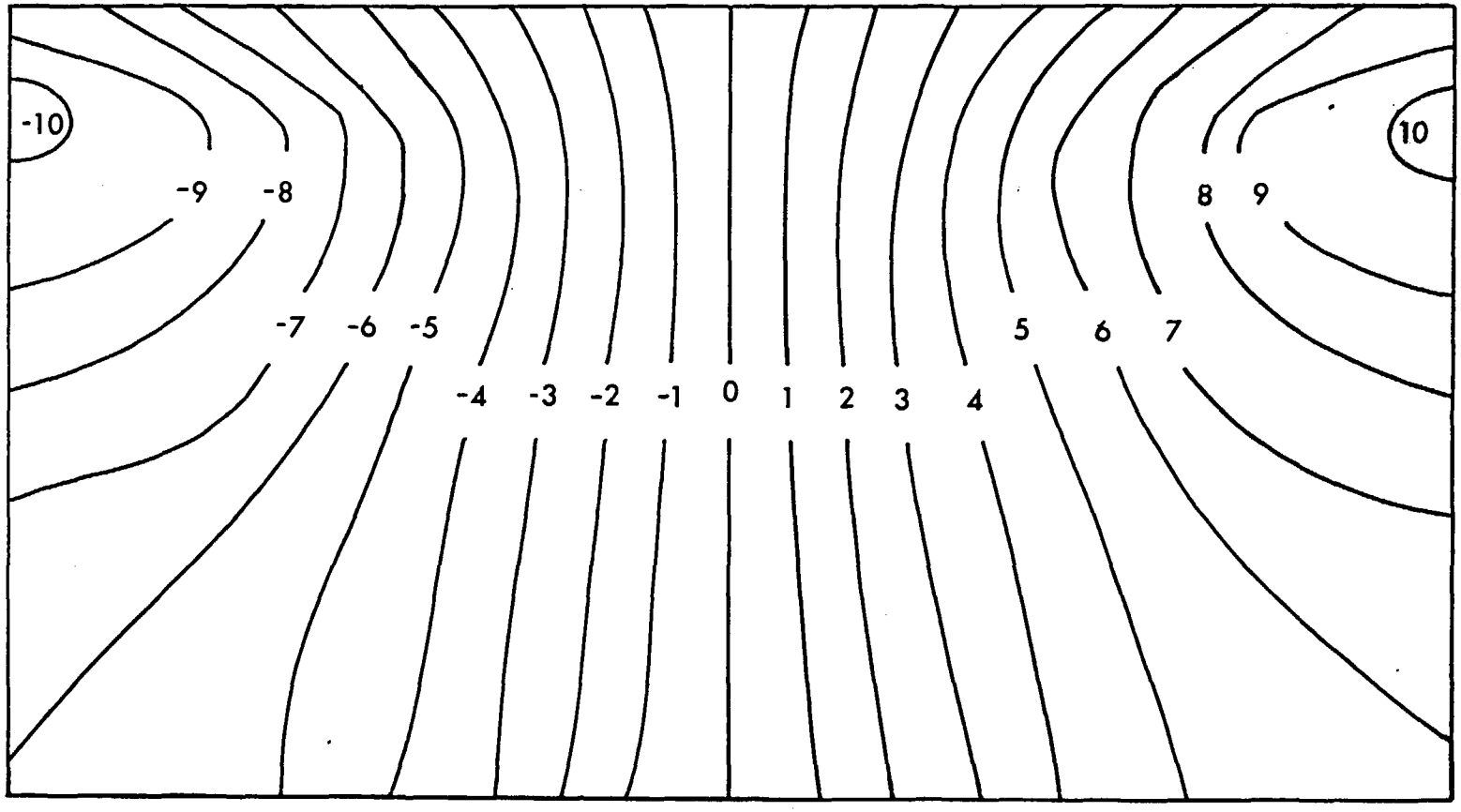

Data Times 100

Figure 7

UNCONFINED

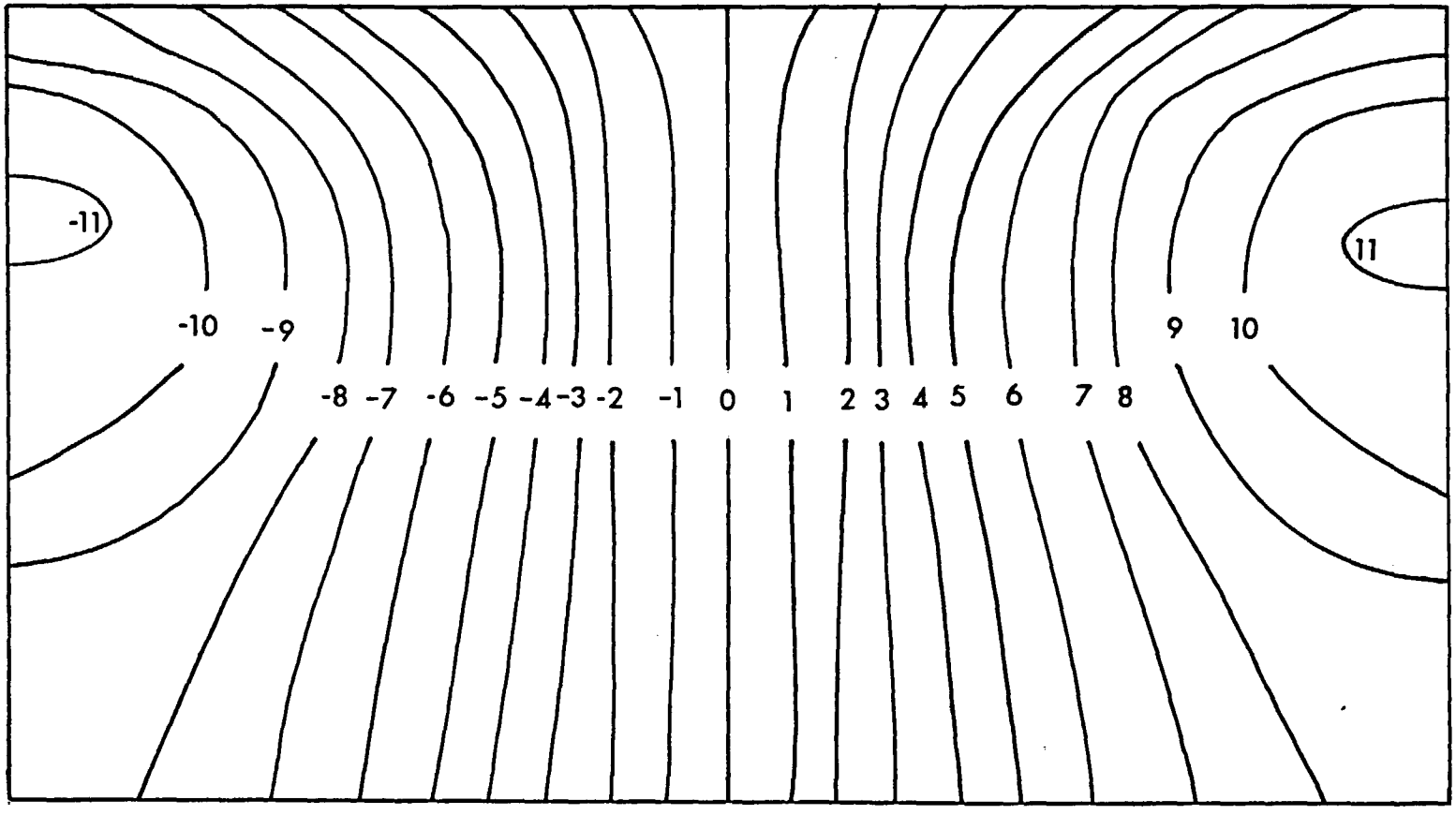

Data Times 100

Figure 8

rather than penetrate the more impermeable lower half. The average absolute value of the correction matrix is 6.099%; the highest value of any node is 11.028%. These are the largest values computed for any of the three example correction factors.

The correction matrix for the confined case is contoured in Figure 9 and the data presented in Appendix B, Table 6. The upper hydraulic conductivity is 1.0 and the lower hydraulic conductivity is 100.00. This induces a greater amount of flow in the Y direction and changes the configuration of the correction matrix to a significant extent. Virtually all of the correction is concentrated in the upper part of the matrix, and the average values are lower than in either of the other example correction factors. Figure 9 also shows that a correction factor is not necessarily needed in a confined case. The average value of the correction matrix is only 1.592%; the largest absolute value at any node is 8.217%. The computer programs used to generate the correction matrices are listed in Appendix D.

GEOLOGY AND HYDROGEOLOGY FROM PAHUTE MESA TO YUCCA FLAT, NEVADA TEST SITE

Introduction

To apply the newly-developed correction factor to a real-world situation, an area of the Nevada Test Site was chosen to model (see Figure 10). A water table map of the Nevada Test Site (Fenske and Carnahan, 1975) displays several recharge-discharge systems. The majority of nuclear device testing takes place at Pahute Mesa (a recharge area), Rainier Mesa (next to Pahute Mesa), and Yucca Flat (a regional sink). Since this project is part of the continuous research of water movement at the Test Site, it was decided to model the area between Pahute Mesa and Yucca Flat. The lines a, b, and c between points A-A' are normal to the water table and are representative flow paths (see Figure 11). The line b positions the model between Pahute Mesa and Yucca Flat. Lines 1 and 1' are the outer boundaries of water flow in the Pahute Mesa-Rainier Mesa-Yucca Flat groundwater system.

The geology in this area is known from surface studies, and from geophysical logging of test and emplacement wells. Hydrogeologic data were taken from the well

CONFINED

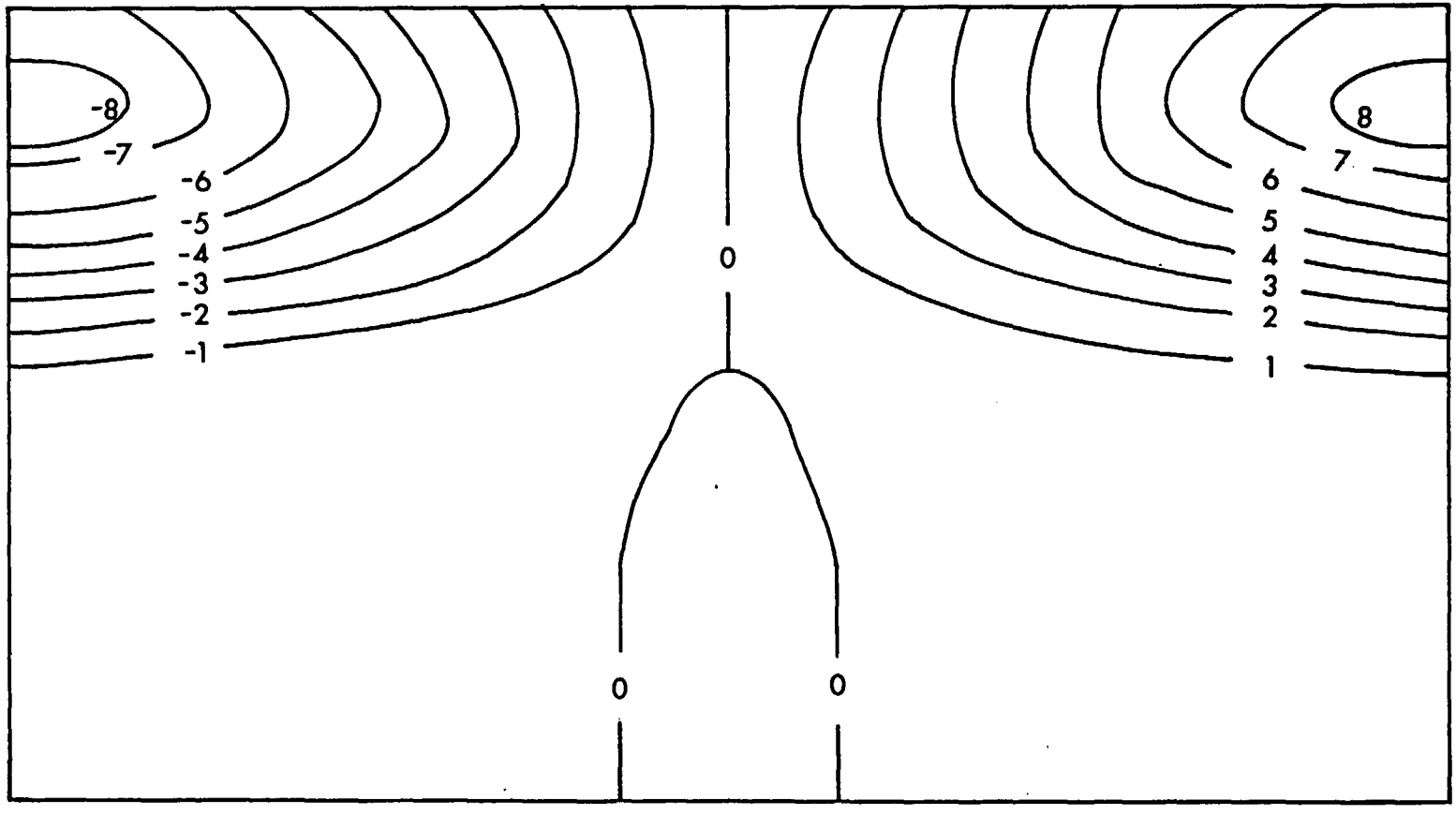

Data Times 100

Figure 9

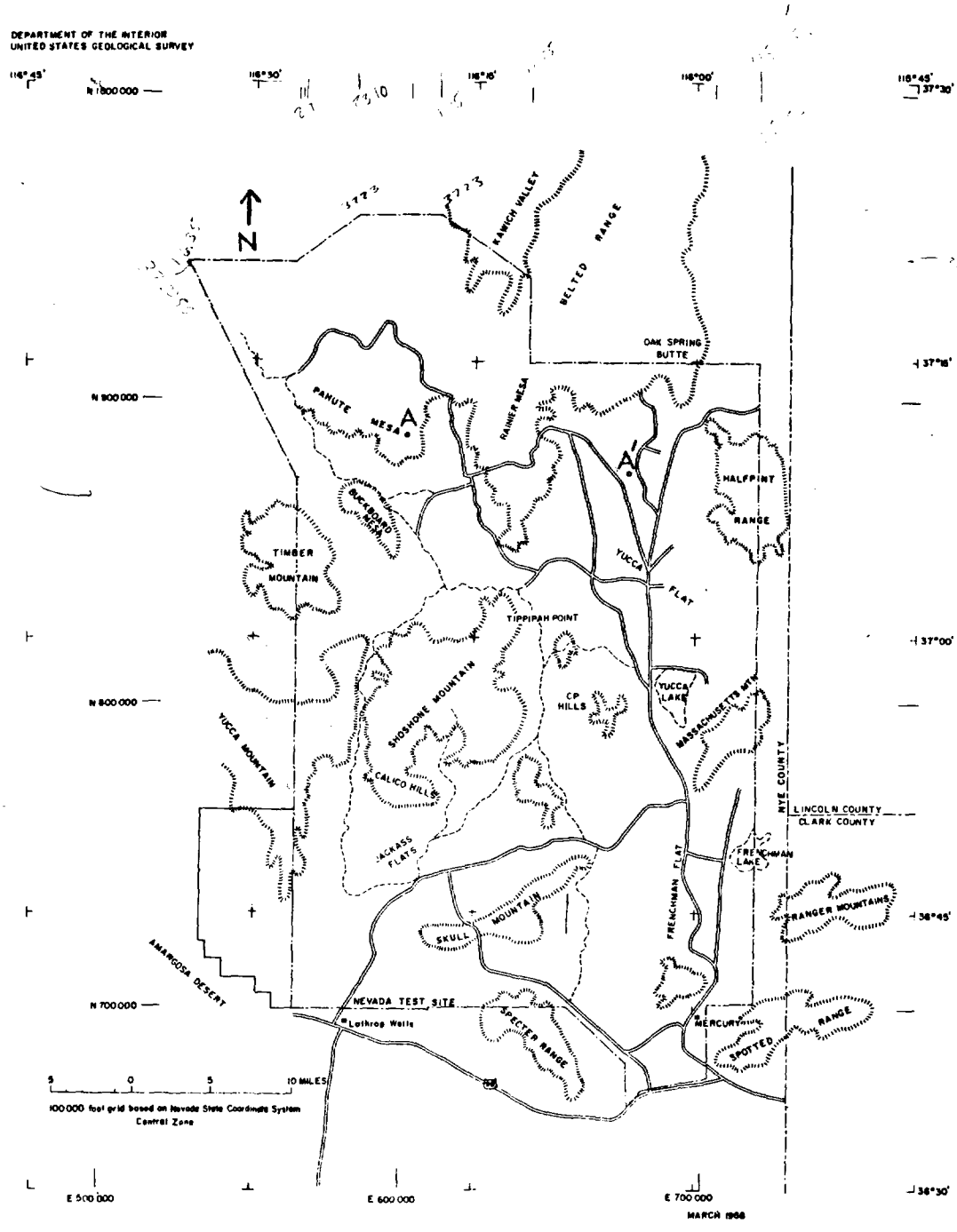

Figure 10. Index to generalized topographic features in the Nevada Test Site and vicinity.

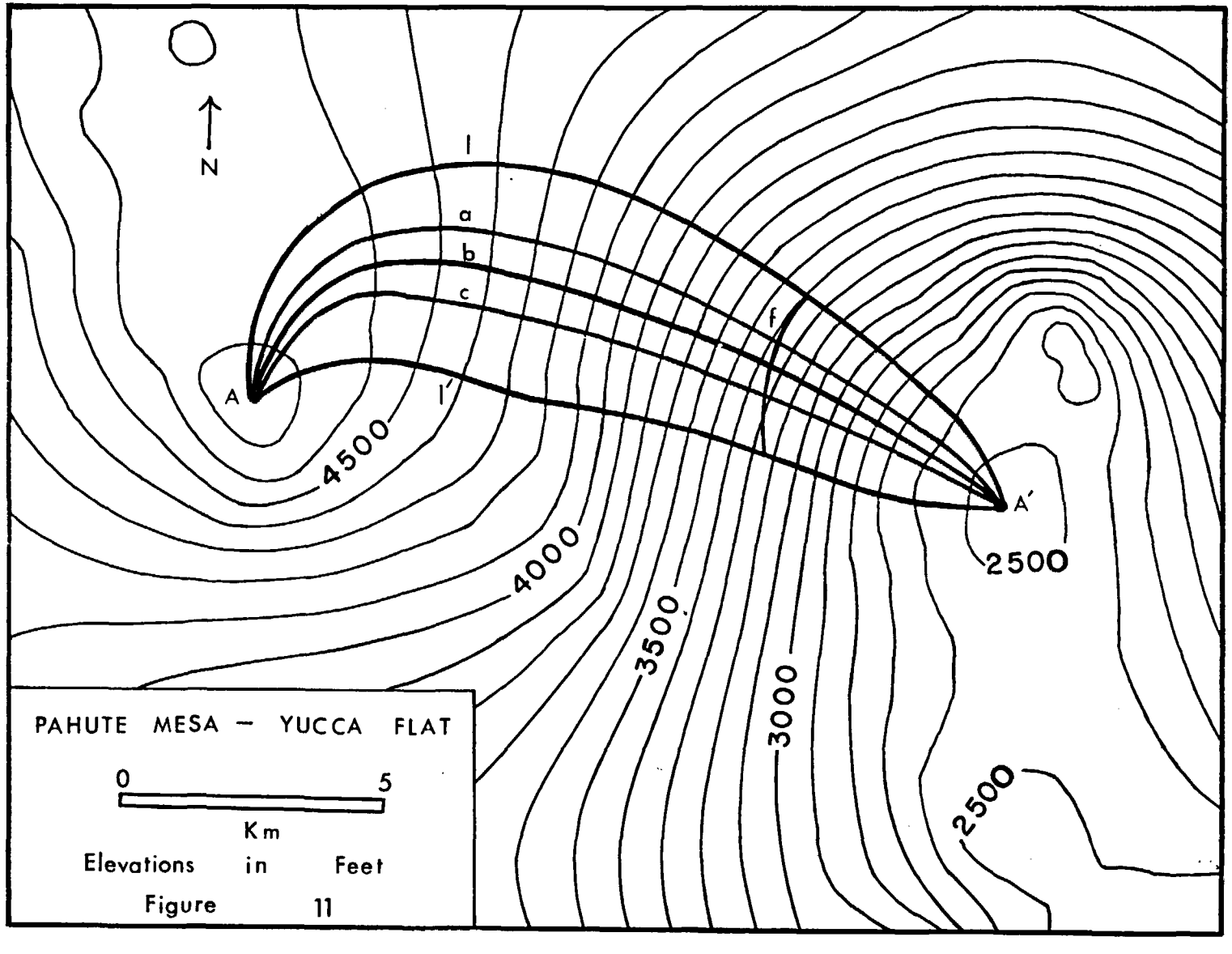
N
l
a
b
c
f
l′
A
A′
4500
4000
3500
3000
2500
2500
PAHUTE MESA — YUCCA FLAT
0
5
Km
Elevations in Feet

Figure 11

tests done at the Test Site. The Theis method was used to compute the values of hydraulic conductivity. In many rock units there are no data because a) the water table is below the rock unit at that well, b) the unit is not considered a major aquifer and is sealed off with casing, or c) no wells are drilled in the rock unit. In these areas, estimates of hydraulic conductivity were made from average values in similar rock types taken from Linsley et al., (1975) and Davis and DeWiest (1966). Geological and hydrogeological data are from Winograd et al., (1971) and Barnes et al., (1963b). In some instances there are estimates for transmissivities for units or a group of units. Where these values were available, they were used to check the estimates made from rock type only.

Regional Geologic Setting

The Nevada Test Site is geologically complex. The area lies within the miogeosynclinal belt of the Cordilleran geosyncline. During the Precambrian and Paleozoic eras, over 11,000 meters of marine sediments accumulated. The region was subjected to two major periods of deformation. The first orogeny occurred in late Mesozoic and resulted in folding and large scale thrust faulting of the Precambrian and Paleozoic rocks. In late Cenozoic, the region experienced normal block-faulting, which produced a superb example of Basin and Range topography.

The rock units found in the Pahute Mesa-Yucca Flat area range from late Precambrian quartzites to Quaternary basalts. The composite thickness of these units is greater than 13,000 meters (see Table 1). The Mesozoic rocks are limited to intrusive bodies of quartz monzonite and granodiorite. Cenozoic rocks consist of tuffs and lava flows. The total thickness of the Cenozoic in the Yucca Flat area is over 1000 meters. In most cases these volcanics were deposited on a deeply-eroded Paleozoic surface.

Rock Units and Associated Hydraulic Conductivities

PRECAMBRIAN ROCKS

Jonnie Formation

The Jonnie Formation is widely exposed in the northern Halfpint Range northeast of Yucca Flat. The formation was also found at depth in thrust sheets in UE15d and Exploratory #1 drill holes near the northwest part of Yucca Flat.

Table 1

ERA	PERIOD	SYMBOL	UNIT NAME	ESTIMATED AND MEASURED HYDRAULIC CONDUCTIVITIES IN m day^{-1}
Cenozoic	Quaternary	Qal	Alluvium	above saturated zone
		Qac	Alluvium-Colluvium	above saturated zone
	Tertiary	Titpc	Indian Trail and Piapi Canyon Formations Undifferentiated	1.00×10^{-2}
		Tpr	Piapi Canyon Formation Rainier Mesa Member	above saturated zone
		Tps	Survey Butte Member	"
		Tigl	Indian Trail Formation Grouse Canyon Member	"
		Tilt	Lower Member	1.00×10^{0}
		Trq	Rhyolite Flows of Quartet Dome	4.08×10^{0}
		Tbb	Unnamed Bedded Airfall Tuff	3.30×10^{-1}
		Trs	Rhyolite of Split Ridge	3.50×10^{0}
		Tcf	Tuff of Crater Flat	5.25×10^{-1}
		Tf	Fraction Tuff	5.00×10^{-1}
		Tb	Unnamed Bedded Tuff	5.00×10^{-3}
Meszoic	Cretaceous	Mc	Unnamed Conglomerate	3.00×10^{1}
	Jurassic-Triassic	KJqm	Quartz Monzonite of Gold Meadows Stock	4.08×10^{-4}

Table 1 (continued)

ERA	PERIOD	SYMBOL	UNIT NAME	ESTIMATED AND MEASURED HYDRAULIC CONDUCTIVITIES IN m Day^{-1}
Paleozoic	Pennsylvanian Mississippian	PMe	Eleana Formation	5.00×10^{-5}
	Devonian Silurian	Ddg	Devils Gate Formation	1.95×10^{-2}
		Dn	Nevada Formation	1.95×10^{-2}
		DSOI	Undifferentiated Devonian, Silurian, Ordovician Dolomite	1.30×10^{-1}
	Ordevician Silurian	Oe	Eureka Quartzite	4.00×10^{-4}
		Opa	Antelope Valley Formation	2.85×10^{-2}
		Opn	Nine Mile Formation	6.56×10^{-2}
		Opg	Goodwin Formation	6.56×10^{-2}
	Cambrian	θw	Windfall Formation	2.41×10^{-1}
		θd	Dunderberg Shale	1.00×10^{-4}
		θbk	Bonanza King Formation	2.26×10^{-1}
		θc	Carrara Formation	5.10×10^{-2}
		θz	Zabriskie Quartzite	4.10×10^{-4}
		θwc	Wood Canyon Formation	4.10×10^{-4}
Precambrian		pθst	Stirling Quartzite	4.10×10^{-4}
		pθj	Jonnie Formation	2.00×10^{-3}

The Jonnie Formation in the Halfpint Range is composed of more than 850 meters of quartzite and siltstone, with minor silty limestone and dolomite, and is believed to be late Precambrian in age. It has not been hydraulically tested at the Nevada Test Site; it is given an average hydraulic conductivity of 2.0×10^{-3}m day^{-1}.

Stirling Quartzite

Stirling Quartzite, northeast of Yucca Flat, contains about 870 meters of quartzite with minor siltstone and micaceous quartzite. Basal contact of the Stirling Quartzite appears to be a bedding plane fault. There is probably very little loss in stratigraphic thickness along the fault, but the underlying Jonnie Formation is locally deformed and commonly nonconformable to the Stirling. There are no well tests of the Stirling at depth and an average hydraulic conductivity of 4.1×10^{-4}m day^{-1} has been assigned. No fossils have been found in the Stirling Quartzite, but its regional stratigraphic position indicates it is of late Precambrian age.

CAMBRIAN (?) AND CAMBRIAN ROCKS

Wood Canyon Formation

Wood Canyon contains about 715 meters of micaceous quartzite, micaceous siltstone, and shale. All outcropping sequences in the Yucca Flat area are small and truncated by faulting, but all parts of the stratigraphic section exposed can be fit together fairly well. The Wood Canyon is transitional with the overlying Zabriskie Quartzite. Hydraulic conductivity of the Wood Canyon has not been determined by test methods, but is given an average value of 4.1×10^{-4}m day^{-1}. The Wood Canyon is in part Cambrian, based on fragments of olenellid trilobites. The lower two-thrids of the formation is designated as Cambrian(?), but may be Precambrian.

Zabriskie Quartzite

Zabriskie Quartzite consists of 50 meters of massive quartzite. In the Yucca Flat area, the Zabriskie occurs in small faulted outcrops in the Halfpint Range. Since no water wells penetrate the Zabriskie, an average hydraulic conductivity of 4.1×10^{-4}m day^{-1} has been assigned. The Zabriskie Quartzite is dated to Early Cambrian age because it is underlain and overlain by rocks of known Early Cambrian.

Carrara Formation

In the Halfpint Range, the Carrara Formation is about 600 meters of interbedded siltstone and limestone and is Early and Middle Cambrian in age, based on fossil evidence. The lower half of the formation is mainly siltstone and the top half is predominantly limestone. No wells in the Yucca Flat area reach the Carrara Formation. Hydraulic conductivity is estimated at 5.1×10^{-2}m day^{-1}.

Bonanza King Formation

The Bonanza King Formation on the east side of Yucca Flat has a total thickness of about 1400 meters and consists of alternating beds of dolomite and limestone. There have been two well tests in this unit in Yucca Flat. Test well # 10 was sealed so that only the Bonanza King Formation was tested; the test resulted in a hydraulic conductivity of 2.26×10^{-1}m day^{-1}. A second test on Army Well # 1, which included two upper units, the Dunderberg Shale and the Windfall Formation, resulted in a mutual hydraulic conductivity of 1.24×10^{-1}m day^{-1}. Since the Dunderberg Shale is an aquiclude, which would lower the hydraulic conductivity, and the Windfall Formation has a slightly lower hydraulic conductivity than the Bonanza King, these figures are in good agreement. The value 2.26×10^{-1}m day^{-1} from well # 10 was used to determine the hydraulic conductivity of the Bonanza King.

Dunderberg Shale

Dunderberg Shale consists of approximately equal thicknesses of shale and lenticular zones of limestone and shale. The Dunderberg is a non-resistant unit in the Yucca Flat area, about 68 meters thick. Permeability is very low, making the Dunderberg an aquiclude. A hydraulic conductivity of 1.0×10^{-4}m day^{-1} was estimated for this unit, and fossil evidence indicates a late Cambrian age.

Windfall Formation

The Windfall Formation in the Yucca Flat area is about 545 meters of limestone and dolomite. The lower unit consists mainly of massive dolomite about 327 meters thick. The Windfall Formation was tested for permeability by test well # 4 (Winograd, 1965). Results indicated a hydraulic conductivity of 2.41×10^{-1}m day^{-1}. Army Well

1 also tested the Windfall and the units below, the Dunderberg Shale and the Bonanza King Formation, and these results indicated a slightly lower hydraulic conductivity of 1.24×10^{-1}m day^{-1}, but well within experimental error. Although fossil evidence is inconclusive, the Windfall Formation is thought to be of late Cambrian age.

ORDOVICIAN ROCKS

Goodwin Limestone

Goodwin Limestone consists of more than 275 meters of light gray limestone with minor silty limestone and is of early Ordovician age, as determined by fossil evidence. It is the bottom-most unit of the Pogonip Group. Contact of the Goodwin with the underlying Windfall Formation is gradational and is determined on the basis of color. Permeability of the Goodwin has been determined from tests made on GWT-2 in Yucca Flat (Moore et al., 1963). Hydraulic conductivity of 6.56×10^{-2}m day^{-1} was found for the entire Pogonip Group.

Nine Mile Formation

The Nine Mile Formation is composed of 102 meters of interstratified, very thin bedded claystone and limestone, with a ratio of claystone to limestone of about 80 to 20. It is the middle unit of the Pogonip Group. Contact with the underlying Goodwin Limestone is gradational but can be readily mapped. Hydraulic conductivity was determined from well tests on GWT-2 when the entire Pogonip Group was examined (Moore et al., 1963). A value of 6.56×10^{-2}m day^{-1} was used to model this unit. The Nine Mile is abundantly fossiliferous and is early Ordovician in age.

Antelope Valley Limestone

Antelope Valley Limestone is the uppermost formation in the Pogonip Group and dates to middle and early Ordovician. It is about 410 meters thick at Yucca Flat and consists of limestone with some silty limestone. Permeability of this unit was tested in two wells. Hydraulic conductivity of the Pogonip Group is 6.56×10^{-2}m day^{-1}, as determined from well # 3 (Moore et al., 1963). Well GWT-2, which only reaches the upper Pogonip Group, has a hydraulic conductivity of 2.85×10^{-2}m day^{-1}. The latter value is used in the groundwater model.

Eureka Quartzite

Eureka Quartzite consists of 107 meters of prominent white quartzite with a middle unit of limestone. Hydraulic properties of the Eureka have not been determined at the Nevada Test Site; an average value of 4.0×10^{-4}m day^{-1} is given this unit. Fossil fauna indicated a middle Ordovician age for the Eureka Quartzite.

ORDOVICIAN, SILURIAN, AND DEVONIAN ROCKS

Undifferentiated Limestone and Dolomite

In the Rainier Mesa area there is a 640 meter sequence of undifferentiated dolomite, and the age of the unit spans the late Ordovician, Silurian and early Devonian periods. Most of this sequence has not been correlated with established formations outside of the Test Site. The unit consists of dolomite and coarsely crystalline dolomitic limestone. There are no well tests in the Yucca Flat area involving this unit. An average hydraulic conductivity of 1.3×10^{-1}m day^{-1} is estimated.

DEVONIAN ROCKS

Nevada Formation

The Nevada Formation in the Rainier Mesa area consists of about 610 meters of dolomite. The unit varies from finely to coarsely crystalline, laminated to thick bedded. Secondary white calcite fills fractures and replaces fossils. Well tests were performed on the Nevada Formation and the overlying Devils Gate Limestone at Army Well # 1. Hydraulic conductivity of 1.95×10^{-2}m day^{-1} was found for the two units together. Based on stratigraphic position and fossil evidence, the Nevada Formation is thought to be of middle Devonian age.

Devils Gate Limestone

Devils Gate Limestone is 407 meters thick on the east flank of Shoshone Mesa and is composed of limestone and dolomite. It is thought to be of late middle and early late Devonian. Contact of Devils Gate and underlying Nevada Formation is gradational. A well test of the Devils Gate Formation and the Nevada Formation at Army Well # 1 resulted in a combined hydraulic conductivity of 1.95×10^{-2}m day^{-1}.

The model changes size in the Y direction in two steps of 500 meters each so that a sloping water table can be accurately represented. The size of the matrix is reduced when less than 50 percent of the area in a 500 meter square is above the water table. The model consists of three adjoining sections: section one is a (7,22) matrix, section two is a (6,23) matrix, and section three is a (5,3) matrix (see Plate 2).

The boundary along the left and right hand sides of the model is assumed to be impermeable. The boundary along the bottom of the model is also impermeable, representing impermeable basement rocks at depth, for a major part of its length. However, under Yucca Flat, the groundwater is draining into permeable Paleozoics and probably entering into the Ash Meadows groundwater system (Winograd et al., 1971). To model the discharge out the bottom of the model, the head value at well GWT-2 near the right hand side of the cross section has been extended. The head value taken from the Paleozoic aquifer (627.0 meters) is used for the entire right hand side and along the bottom of the model under Yucca Flat.

The average hydraulic conductivity for each 500 meter square was computed by a three step process: first, the geology within each 500 meter square was examined and a percentage of each rock unit determined; second, the percentiles were multiplied by the corresponding hydraulic conductivity; and third, the resulting values were totaled. The values for each square are a composite of the hydraulic conductivities within that square.

The hydraulic conductivity at each node is by definition applicable only for one nodal distance in the positive direction. At any node (Y,Z) the hydraulic conductivity for that node extends to nodes (Y+1,Z) and (Y,Z+1). The finite difference equation for any interior (Y,Z) node becomes:

$$\phi(Y,Z) = \tfrac{1}{4}\Big[\phi(Y+1,Z)K(Y,Z) + \phi(Y-1,Z)K(Y-1,Z) + \phi(Y,Z+1)K(Y,Z) + \phi(Y,Z-1)K(Y,Z-1)\Big] \qquad \text{Eq. 13}$$

Where $K(Y,Z)$ = the hydraulic conductivity at node (Y,Z)

Using equation 13, the matrix representing the groundwater system between Pahute Mesa to Yucca Flat was simulated. The model was iterated until a convergence factor of ± 0.0001 was reached.

MISSISSIPPIAN AND PENNSYLVANIAN ROCKS

Eleana Formation

The Eleana Formation in the Yucca Flat area is composed of more than 2350 meters of argillite, siliceous siltstone and very fine-grained quartzite, quartzite and conglomerate, and limestone. Its age, based on stratigraphic position and fossil evidence, is considered to be Mississippian and early Pennsylvanian. In outcropping at Rainier Mesa, the Eleana Formation is folded and overturned. No wells at the Nevada Test Site in the Eleana reach the water table. The average hydraulic conductivity for an argillaceous limestone is estimated at 5.0×10^{-4}m day^{-1}.

MESOZOIC ROCKS

Gold Meadows Stock

Gold Meadows Stock is a quartz monzonite intrusive that outcrops over an area of 3.8 square kilometers in the northern part of Rainier Mesa. The stock consists of an estimated 80 percent quartz monzonite, 15 percent porphyritic quartz monzonite, and 5 percent aplite and pegmatite. Texture of the quartz monzonite is medium to coarse-grained. Geophysical studies indicate that the stock slopes at about 45 degrees to the southwest (Barnes et al., 1963). Hydraulic conductivity for the stock was estimated from data on quartz monzonites of the Colorado Front Range (Davis and Turk, 1964); a value of 4.08×10^{-4}m day^{-1} has been estimated for this unit. Age of the Gold Meadows stock, determined by lead-alpha analysis of zircon, ranges from late Jurassic to late Cretaceous.

Unnamed Conglomerate

An unnamed and discountinuous conglomerate rests on the deeply eroded Paleozoic and Mesozoic surface. It ranges from 0 to 75 meters thick. No permeability tests have been done on this unit, and an average value of 3.0×10^{1}m day^{-1} is assumed.

TERTIARY ROCKS

Unnamed Bedded Tuff

In the southern part of Pahute Mesa, well GWT-8 encountered an unnamed bedded tuff, 61 meters thick and consisting mainly of zeolitic bedded tuff. This unit overlies

eroded Paleozoics and Mesozoic conglomerate. Hydraulic conductivity of zeolitic tuffs is quite low (Blankennagel and Weir, 1973), and a value of 5.0×10^{-3}m day^{-1} has been estimated for this unit. Age of the unnamed bedded tuff is Miocene or younger.

Fraction Tuff

Fraction Tuff consists of about 400 meters of ash-fall tuff and tuffaceous sandstone and is a part of the lower unit of the Indian Trail Formation. In some areas the Fraction Tuff rests on the Paleozoic surface. Hydraulic conductivity of 5.0×10^{-1}m day^{-1} has been estimated for this unit.

Tuff of Crater Flat

The Tuff of Crater Flat consists of 275 meters of welded tuff and is part of the Indian Trail Formation. Well GWT-8 penetrated this unit, and well tests were performed on the Tuff of Crater Flat, the overlying Rhyolite of Split Ridge, and an unnamed bedded air-fall tuff. Hydraulic conductivity of the Tuff of Crater Flat is 5.25×10^{-1}m day^{-1} (Winograd, 1965).

Rhyolite of Split Ridge

Rhyolite of Split Ridge ranges from 0 to 335 meters thick and consists largely of flows and dikes of thinly flow-laminated phenocryst-poor rhyolite; some flows are columnar and fan jointed. Rhyolite of Split Ridge interfingers with an overlying unnamed bedded air-fall tuff. Hydraulic conductivity was determined from well tests of GWT-8 (Winograd, 1965); a value of 3.50m day^{-1} is taken from test data.

Unnamed Bedded Air-fall Tuff

The unnamed bedded air-fall tuff varies from 0 to 520 meters of zeolitic fine to lapilli tuff and commonly underlies the Grouse Canyon Member. The unit is generally intercalated between flow of Rhyolite of Split Ridge. Well tests at GWT-8 yield a hydraulic conductivity of 3.3×10^{-1}m day^{-1}.

Rhyolite Flows of Quartet Dome

The Rhyolite Flows of Quartet Dome range from 0 to 243 meters of thickly and roughly flow-layered porphyritic rhyolite. Values for hydraulic conductivity are estimated from similar rhyolites of Pahute Mesa, and a figure of 4.0 m day^{-1} is used in modeling this unit.

Indian Trail Formation

In the northern and central parts of the Yucca Flat-Rainier Mesa area, the volcanic rocks in the lower half of the Tertiary section are called the Indian Trail Formation. The formation has a maximum thickness of 580 meters and is subdivided into three members: an informal lower member, the Tub Spring Member (not always present), and the Grouse Canyon Member.

Lower Member

The lower member, an informal unit, has a thickness that ranges from 43 meters to 183 meters and contains rhyolitic tuffs, rhyolite, tuffaceous siltstone and tuffaceous sandstone. The lithology varies from one locality to another and cannot be correlated with assurance. In many places this unit rests on the eroded Paleozoic-Mesozoic surface. No hydraulic tests have been performed on this unit; hydraulic conductivity of 1.0 m day^{-1} is estimated.

Grouse Canyon Member-Lower Part

The lower part of the Grouse Canyon Member ranges from 43 meters to 122 meters of nonwelded bedded tuff. Contact of the Grouse Canyon Member with underlying units is conformable in most places on Rainier Mesa. The Grouse Canyon Member is a widespread unit that can be located over most of Yucca Flat. It is above the water table and a hydraulic conductivity has not been assigned.

Piapi Canyon Formation

The Piapi Canyon Formation is found throughout the Yucca Flat area and ranges in thickness from 400 to 490 meters. The lower contact of the formation is well exposed throughout much of the northwestern part of Yucca Flat, where it is separated by an erosional unconformity from the tuffs of the Indian Trail Formation.

Survey Butte Member

The Survey Butte Member consists of 30 to 305 meters of ash-fall tuff. Locally this unit has been reworked by wind and water. The Survey Butte Member beds are poorly cemented and friable, with some cross-beds and channel fillings. The lower 30 meters has been zeolitized locally. This unit is above the regional water table and was not modeled.

Rainier Mesa Member

Rainier Mesa is composed of tuffs which cap Rainier Mesa. It includes the youngest ash-flow tuff exposed in the Yucca Flat area and is the most widespread

Structures

Examination of the landforms of the Yucca Flat area suggests that the structural pattern is mainly a result of basin and range faulting. The most complex structures are the buried Paleozoic and Precambrian rocks under Yucca Flat and Rainier Mesa. These rocks have been folded, cut by high-angle and thrust faults, folded again, and cut again by high-angle faults. Rocks of Tertiary age are cut by many conspicuous high-angle faults and in places are warped into broad folds (see Plate 1).

There are four, and possibly, five major thrust faults in the Yucca Flat area. The area of Yucca Flat studied for this paper contains two known and one inferred thrust fault. The movement of these thrusts is to the east, with a horizontal displacement on the order of 10 to 16 kilometers. The eastern-most thrust carried the Eleana Plate (composed mainly of the Eleana Formation) over northeast-trending broadly folded Paleozoics.

The next thrust fault west is the Mine Mountain Thrust Fault. This thrust carried older Paleozoics of Devonian, Silurian and Ordovician age over younger Paleozoics of the Eleana Plate. The Eleana Plate is highly deformed by the thrust and contains many faults and folds, and is overturned over a large area in an inverted syncline. The third possible thrust fault underlies Rainier Mesa and is based on the evidence from a single drill hole, 0126-07-2. It appears that the Precambrian Jonnie (?) Formation is thrust over Early Paleozoics. The Gold Meadows Stock intrudes this thrust, called the Jonnie Thrust herein, and the continuation of the thrust on the opposite side of the stock is purely speculative.

There are three large-scale normal faults in the area of the cross section. All three are well studied and their position and magnitude of offset is reliable. The eastern-most is the Tippinip Fault, which divides Yucca Flat structurally into an eastern and western block. The rocks in the eastern block are largely folded Paleozoic and Precambrian rocks. The structure in the western block consists of Tertiary volcanics covering folded and thrust faulted Paleozoic rocks. The Tippinip Fault has a vertical displacement of about 310 meters.

The next major normal fault to the west is the Boundary Fault, with an offset of ca. 340 meters, which cuts through Paleozoic rocks and the front of the Eleana Plate. The fault is traceable to the north for over 16 kilometers and to the south for about 10 kilometers.

The western-most major normal fault is an unnamed fault that offsets the Eleana Plate and the Mine Mountain thrust. The fault can be traced north past Survey Butte and to the southwest to Tongue Wash. The estimated vertical displacement is 520 meters.

There are hundreds of mappable normal faults in the Yucca Flat-Rainier Mesa area, and many more are covered by alluvium. Since 45 percent of the area in this cross section is covered by alluvium and colluvium, a large number of faults with small offsets have not been mapped. Geophysical studies have determined the depth to bedrock in Yucca Flat, but the nature of the bedrock is unknown (Healey, 1965). The structural position of the buried bedrock has been interpolated from other areas; however, numerous small faults undoubtedly alter these units in an unknown manner.

To the east of Gold Meadows Stock the eroded Paleozoic surface is buried under thousands of feet of rhyolite and bedded air-fall tuff. Faults in the Paleozoic bedrock are also similarly present but obscured.

The largest single structure in the cross section is the Gold Meadows Stock. The stock has been delineated by gravity studies and its general form is known (Snyder, 1977). At depth, however, the extent of the intrusive has been estimated. All geology west of the stock, except surface geology, is speculative, because of lack of geological data at depth. The presence of the Jonnie Thrust in this area is one of several possible solutions. The well GWT-8 projected at the western part of the cross section is over three kilometers to the southeast, and extension of the geology is based on a most likely situation (Healey et al., 1963).

GROUNDWATER MODEL OF PAHUTE MESA TO YUCCA FLAT

In order to mathematically model the hydrogeology of the cross section a finite difference computer program was written that incorporates hydraulic conductivities and the aforementioned correction matrix. The cross section is divided into 307 sections, each of which is 500 meters square. The nodal spacing is based on the distance between nodes (610 meters) used to calculate the water table (Carnahan and Fenske, 1971). A nodal spacing any smaller than 500 meters cannot be justified because of the resolution to which the water table was computed. The head values at nodes representing the water table are taken from Fenske and Carnahan (1975).

The correction matrix applied to the groundwater model was computed using an upper hydraulic conductivity of 4.86 and a lower hydraulic conductivity of 1.0. These values have the same ratio to each other as the actual values and hence give identical results. The actual values of 0.3254 m day^{-1} for the upper layer and 0.0669 m day^{-1} for the bottom layer were not used in order to decrease computer time, and to use a form comparable to other correction matrices computed.

The correction matrix was developed for applicability to the average recharge-discharge system, i.e., a spring discharging at the base of a range. However, groundwater flow at Yucca Flat flows downward into the Paleozoic aquifers. To model these special conditions, the correction matrix was recomputed after modifying the matrices Box and Mat to allow water to discharge out the bottom. This was done by assuming water table conditions along the bottom of the right hand portion of the matrices. The initialized head values for the water table are from 20.0 to 12.63 in the recharge surface values and 12.11 to 10.0 in the discharge bottom values. The ratio of recharge area to discharge area is the same as in the Pahute Mesa-Yucca Flat groundwater model, or 4 to 1, respectively.

The correction matrix for the Pahute Mesa-Yucca Flat groundwater model is shown contoured in Figure 12. The scale of the figure is the same as that of the other correction matrices for purposes of comparison. The value of the correction matrix applied to the Pahute Mesa-Yucca Flat area is given in Table 7. Average value of the correction matrix is 5.889%; highest value at any node is 11.9%. Configuration of the matrix is significantly altered by flowing the water out of the bottom of the model. It is not symmetric because of the smaller length of the lower discharge area. Average value of the correction matrix is 8.79% above the lower discharge area and 3.04% below the recharge area.

The head potential model for the Pahute Mesa-Yucca Flat groundwater system is shown in Plate 2. Data for Plate 2 are listed in Table 7, Appendix B. Examination of Plate 2 shows several interesting features: first, the left hand portion of the model has little change in head potential, due to the concentration of relatively impermeable quartzites and monzonites in this area. Second is the curvature of the 1200 meter equipotential line. The upper part of the line indicates there is a small amount of

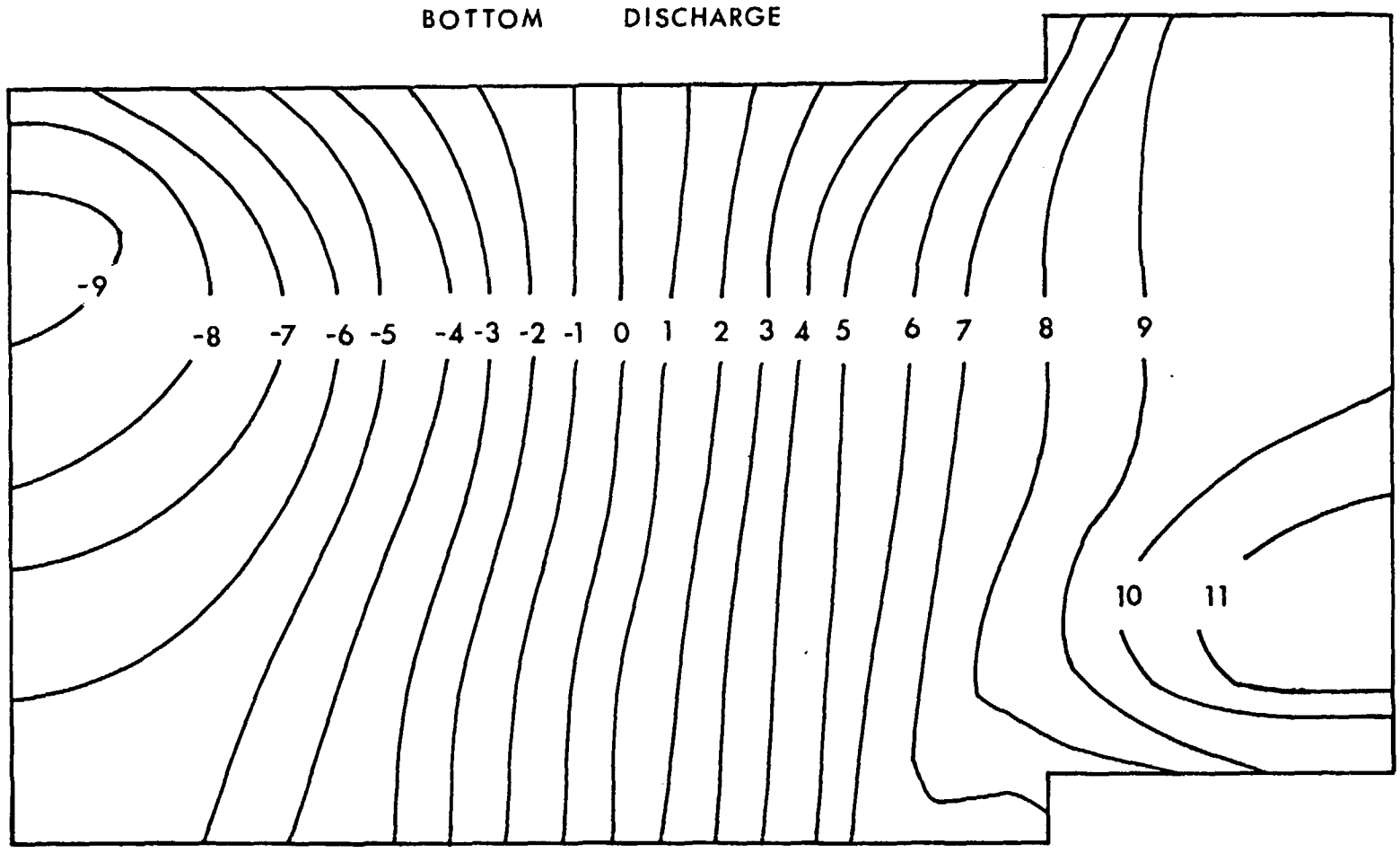

Data Times 100 Figure 12

discharge (or if no discharge, an upward bulge in the water table) at that point. This is caused by the impermeable Eleana Formation blocking the flow of groundwater and forcing some of the water upwards. Third is the hydraulic barrier caused by the Eleana Formation. This is clearly seen in the closely-spaced equipotential lines 1200 meters through 800 meters. Fourth, the major part of the recharge seems to be taking place at Pahute Mesa. This is seen by the distance between the equipotential lines and the higher head values.

In order to better interpret the model, four representative flow paths are plotted. These lines show the path the water would most likely take. Flow lines are assumed to always be perpendicular to equipotential lines. The volume of water flowing into the lower Paleozoic aquifers can be computed from this model. Since the volume of water between two flow lines is the same for each potential drop, a relatively simple formula can be used to calculate discharge.

For the flow between any two flow lines along an equipotential line:

Q = (average gradient) (average hydraulic conductivity) (distance between flow lines along single equipotential line) Formula 1

Using this method, the flow between each pair of flow paths along the 900 meter equipotential line was computed based on the 500 meter grid system. The flow through channels 1, 2 and 3 is listed below.

Flow channel 1	33.2 m^3 day^{-1}
Flow channel 2	30.8 m^3 day^{-1}
Flow channel 3	149.7 m^3 day^{-1}

The combined flow equals 213.7 m^3 day^{-1} or 64.8 acre feet $year^{-1}$.

The outermost flow lines, 1 and 1' in Figure 11, show the maximum size of the Pahute Mesa-Rainier Mesa-Yucca Flat groundwater system. The fault boundary between Yucca Flat and the Eleana Plate can be interpolated, line f, between flow lines 1 and 1'. The area bounded by these lines (15.1Km^2) is the part of Yucca Flat where the water from Pahute Mesa is flowing into the deep Paleozoic aquifers. Knowing the volume of water flow per day and the area of its flow, the rate of flow is computed at 14.1 m^3 day^{-1}/Km^2 in this portion of Yucca Flat. If this rate is applied to all of Yucca Flat, 295 Km^2, the volume of water flowing into the Ash Meadows groundwater system is 4175 m^3 day^{-1}, or 1240 acre feet $year^{-1}$. This value must be considered as the maximum possible flow under Yucca Flat because conditions for groundwater

recharge are best at Pahute Mesa. This figure is in fair agreement with Winograd et al. (1971), who estimated the total discharge for all of Yucca Flat at less than 350 acre feet/year. The model computes the discharge only for the northern one-eighth of the area in Winograd's estimate. The amount of flow between Pahute Mesa and Yucca Flat is probably reasonably close to the actual value; however, there have been several assumptions made: the shape of the water table, the geology, the structure, some of the hydraulic conductivities, and the nature of the correction factor. For these reasons, the author believes that the computed flow may be as much as ± 50% of the actual value. The volume of water beneath Yucca Flat that flows into the Ash Meadows groundwater system is probably less than half of the maximum value given.

CONCLUSIONS

Two dimensional finite difference models can be partially corrected for flow in the lateral direction. The correction factor is greatest for unconfined cases and averages 6.1% when the upper layer hydraulic conductivity is 100 times the lower layer. The correction factor has the least value in a confined case. A lower layer with a hydraulic conductivity 100 times greater than the upper layer has an average correction of 1.6%. The correction factor for a homogeneous medium averages 4.9%. The major part of the correction factor is concentrated in the recharge and discharge areas. Since computations concerning flow rates are usually computed in these areas, the correction matrix can have a significant effect and is best applied in an unconfined situation to models with very accurate geological and hydrogeological input data.

Groundwater flow rate into the Paleozoic rocks beneath Yucca Flat is about 14.1 m^3 day^{-1}/Km^2 between Pahute Mesa and Yucca Flat. A maximum of 4175 m^3 day^{-1} of water enters the Ash Meadows groundwater system from Yucca Flat. The area between Pahute Mesa and Yucca Flat is nearly all recharge area, with the major part of the recharge taking place at Pahute Mesa. Further mathematical treatment of the model would be needed to more fully understand the direction and volume of groundwater in this area.

BIBLIOGRAPHY

Barnes, Harley, 1962, Maximum Thickness and Principal Lithology of Rocks, Yucca Flat Area, Nevada Test Site: U.S. Geological Survey Technical Letter: Yucca-35, 4 pp.

Barnes, Harley, Houser, Fred N., and Poole, Forrest G., 1963a, Geologic Map of the Oak Springs Quadrangle, Nye County, Nevada: U.S. Geological Survey Geol. Quad. Map GQ-214.

Barnes, Harley, Hinrichs, E. Neal, McKeown, F.A., and Orkild, Paul P., 1963b, U.S. Geological Survey Investigations of Yucca Flat, Nevada Test Site, Part A-Geology of the Yucca Flat Area: U.S. Geological Survey Technical Letter: NTS-45, Part A, 196 pp.

Blankennagel, R.K., and Weir, J.E., Jr., 1966, Well Histories and Drilling Data on Exploratory Test Holes, Pahute Mesa, Nevada Test Site: U.S. Geological Survey Technical Letter: Special Studies-I-46, 5 pp.

Blankennagel, Richard K. and Weir, J.E., Jr., 1973, Geohydrology of the Eastern Part of Pahute Mesa, Nevada Test Site, Nye County, Nevada: Geological Survey Professional Paper 712-B, 35 pp.

Boas, Mary L., 1966, Mathematical Methods in the Physical Sciences: New York, John Wiley & Sons, Inc., 778 pp.

Carnahan, Chalon L., and Fenske, Paul R., 1975, An Empirical Method for Simulation of Water Tables by Digital Computers: Desert Research Inst., University of Nevada, NVO-1253-7, 29 pp.

Carnahan, C.L., and Fenske, P.R., 1971, Digital Computer Simulation of Water Table: Desert Research Inst., University of Nevada, NVO-1229-173, 41 pp.

Carr, W. J., 1965, Structure Contour Map of the Buried Surface of the Pre-Cenozoic Rocks, Yucca Flat, Nevada Test Site: U.S. Geological Survey Technical Letter: NTS-103, 2 pp.

Corchary, George S., and Dinwiddie, George A., Ed., 1975, Field Trip to Nevada Test Site Prepared by U.S. Geological Survey: U.S. Geological Survey Road Log, 92 pp.

Danilchik, Walter, 1968, The UE12t # 1 Exploratory Drill Hole: Stratigraphy, Lithology, and Physical Properties: U.S. Geological Survey Technical Letter: Area 12-22, 36 pp.

Davis, Robert E., 1961, Thickness Variations in the Oak Spring Formation, Rainier Mesa, Nevada Test Site: U.S. Geological Survey Technical Letter: Shade-1, 6 pp.

Davis, Stanley N., and DeWiest, Roger J.M., 1966, Hydrogeology: New York, John Wiley & Sons, Inc., 463 pp.

Davis, S.N., and Turk, L.J., 1964, Optimum Depth of Wells in Crystalline Rocks: Ground Water, v.2, n.2.

Fenske, Paul R., and Carnahan, Chalon L., 1975, Water Table and Related Maps for Nevada Test Site and Central Nevada Test Area: Desert Research Inst., University of Nevada NVO-1253-9, 18 pp.

Fernald, Arthur T., 1967, Thickness of Surficial Deposits in Yucca Flat, Nevada Test Site: U.S. Geological Survey Technical Letter: NTS-194, 2 pp.

Fernald, Arthur T., 1970, Thickness of Surficial Deposits and Tuff in Yucca Flat, Nevada Test Site: U.S. Geological Survey-474-86, NTS-224, 9 pp.

Freeze, R.A., 1969, Theoretical Analysis of Regional Groundwater Flow: Scientific Series No. 3, Inland Waters Branch, Department of Energy, Mines and Resources, Ottawa, Canada, 147 pp.

Freeze, R. Allan, and Witherspoon, P.A., 1966, Theoretical Analysis of Regional Groundwater Flow: Analytical and Numerical Solutions to the Mathematical Model: Water Resources Research, v. 2, n. 4, pp. 641-656.

Freeze, R. Allan, and Witherspoon, P.A., 1967, Theoretical Analysis of Regional Groundwater Flow: Effect of Water Table Configuration and Subsurface Permeability Variation: Water Resources Research, v. 3, n. 2, pp. 622-634.

Freeze, R. Allan, and Witherspoon, P.A., 1968, Theoretical Analysis of Regional Groundwater Flow: Quantitative Interpretations: Water Resources Research, v. 4, n. 3, pp. 581-590.

Gibbons, Anthony B., Hinrichs, E. Neal, Hansen, Wallace R., and Lemke, Richard W., 1963, Geology of the Rainier Mesa Quadrangle, Nye County, Nevada: U.S. Geological Survey Geol. Quad. Map GQ-215.

Hazlewood, R.M., Healey, D.L., and Miller, C.H., 1963, U.S. Geological Survey Investigations of Yucca Flat, Nevada Test Site, Part B. -Geophysical Investigations: U.S. Geological Survey Tech. Letter: NTS-45, 53 pp.

Healey, D.L., 1965, Detailed Gravity Study of Area 2 and Vicinity, Yucca Flat, Nevada Test Site: U.S. Geological Survey Technical Letter: Yucca-58, 10 pp.

Healey, D.L., Currey, F.E., and Smith, R.C., 1963, Interpretation of Gravity Data in the Vicinity of Ground Water Test Well 8: U.S. Geological Survey Technical Letter: NTS-55, 14 pp.

Hinrichs, E. Neal, 1963, Geology of the Ammonia Tanks Quadrangle, Nye County, Nevada: U.S. Geological Survey Technical Letter: NTS-59, 12 pp.

Hinrichs, E. Neal, 1968, Geologic Structure of Yucca Flat Area, Nevada, in Nevada Test Site, Eckel, E.B., Ed.: Geol. Soc. America Mem. 110, pp. 239-246.

Hinrichs, E. Neal, Krushensky, R.D., and Luft, S.J., 1967, Geologic Map of the Ammonia Tanks Quadrangle, Nye County, Nevada: U.S. Geological Survey Geol. Quad. Map GQ-638.

Huntoon, Peter W., 1972, An Introduction to Finite Difference Methods as Applied to Groundwater Problems: Conservation and Survey Division in Cooperation with the Water Resources Research Institute, University of Nebraska-Lincoln: Open-File Report, 99 pp.

Linsley, Ray K., Jr., Kohler, Max A., and Paulhus, Joseph L. H., 1975, Hydrology for Engineers: New York, McGraw-Hill Book Co., 2nd Edition, 482 pp.

Lohman, S.W., 1972, Ground-water Hydraulics: U.S. Geological Survey Professional Paper 708, 70 pp.

McKay, E.J., 1962, Geology of Yucca Flat Quadrangle: U.S. Geological Survey Technical Letter: NTS-38, 5 pp.

Moore, John E., Doyle, Alan C., Walker, George E., and Young, R.A., 1963, Ground Water Test Well 2, Nevada Test Site, Nye County, Nevada: U.S. Geological Survey Report TEI-836, 73 pp.

Snyder, R.P., 1977, Geology of the Gold Meadows Stock, Nevada Test Site: U.S. Geological Survey-474-179, Area 12-26, 13 pp.

Weir, J.E., Jr., 1967, Geologic and Hydrologic Reconnaissance of the Emplacement Chamber U19c, Pahute Mesa, Nevada Test Site: U.S. Geological Survey Technical Letter: Special Studies I-53, 10 pp.

Williams, W.P., Emerick, W.L., Davis, R.E., and Snyder, R.P., 1963, U.S. Geological Survey Investigations in Yucca Flat, Nevada Test Site, Part C. -The Underground Test Media of Yucca Flat: U.S. Geological Survey Technical Letter: NTS-45, Part C., 251 pp.

Wilmarth, V.R., Houser, F.N., and McKeown, F.A., 1961, Summary of Subsurface Geology in Areas 3 and 12, Nevada Test Site: U.S. Geological Survey Technical Letter: NTS-5, 12 pp.

Winograd, I.J., 1965, Pumping Test Data for Selected Wells, Nevada Test Site and Vicinity: U.S. Geological Survey Technical Letter: NTS-116, 28 pp.

Winograd, Isaac J., and West, Lewis R., 1962, Preliminary Tracer Experiment to Demonstrate Hydraulic Continuity Between Water Wells C and C-1, Yucca Flat, Nevada Test Site: U.S. Geological Survey Technical Letter: NTS-20, 7 pp.

Winograd, I.J., and Young, R.A., 1965, Hydrologic Maps of the Nevada Test Site and Vicinity: U.S. Geological Survey Technical Letter: NTS-130, 2 pp.

Winograd, Isaac J., Thordarson, William, and Young, Richard A., 1971, Hydrology of the Nevada Test Site and Vicinity, Southeastern Nevada: U.S. Geological Survey Open-File Report, 429 pp.

APPENDIX A

Head Values for Theoretical Basin

Table 2

The Area of the Matrix Box Equivalent to the Matrix Mat

Y axis ↓	Z axis → 1	2	3	4	5	6	7	8	9	10
1	20.00	19.47	18.95	18.42	17.89	17.37	16.84	16.32	15.79	15.26
2	17.63	17.49	17.27	17.01	16.72	16.42	16.11	15.80	15.48	15.16
3	16.70	16.65	16.53	16.38	16.20	16.00	15.79	15.57	15.34	15.11
4	16.23	16.20	16.13	16.03	15.90	15.76	15.60	15.44	15.26	15.09
5	15.94	15.93	15.88	15.81	15.71	15.60	15.48	15.35	15.21	15.07
6	15.76	15.74	15.71	15.65	15.58	15.49	15.39	15.29	15.17	15.06
7	15.63	15.62	15.59	15.54	15.48	15.41	15.33	15.24	15.15	15.05
8	15.53	15.53	15.50	15.47	15.42	15.36	15.29	15.21	15.13	15.04
9	15.47	15.46	15.44	15.41	15.37	15.32	15.25	15.19	15.11	15.04
10	15.43	15.42	15.41	15.38	15.34	15.29	15.23	15.17	15.10	15.04
11	15.41	15.40	15.38	15.36	15.32	15.27	15.22	15.16	15.10	15.03
12	15.40	15.39	15.38	15.35	15.31	15.27	15.22	15.16	15.10	15.03

Y axis ↓	Z axis → 11	12	13	14	15	16	17	18	19	20
1	14.74	14.21	13.68	13.16	12.63	12.11	11.58	11.05	10.53	10.00
2	14.84	14.52	14.20	13.89	13.58	13.28	12.99	12.73	12.51	12.37
3	14.89	14.66	14.43	14.21	14.00	13.80	13.62	13.47	13.35	13.30
4	14.91	14.74	14.56	14.40	14.24	14.10	13.97	13.87	13.80	13.77
5	14.93	14.79	14.65	14.52	14.40	14.29	14.19	14.12	14.07	14.06
6	14.94	14.83	14.71	14.61	14.51	14.42	14.35	14.29	14.26	14.24
7	14.95	14.85	14.76	14.67	14.59	14.52	14.46	14.41	14.38	14.37
8	14.96	14.87	14.79	14.71	14.64	14.58	14.53	14.50	14.47	14.47
9	14.96	14.89	14.81	14.75	14.69	14.63	14.59	14.56	14.54	14.53
10	14.97	14.90	14.93	14.77	14.71	14.66	14.62	14.60	14.58	14.57
11	14.97	14.90	14.84	14.78	14.73	14.68	14.64	14.62	14.60	14.60
12	14.97	14.90	14.84	14.78	14.73	14.69	14.65	14.62	14.61	14.60

Table 3

The Matrix Mat

Y axis ↓	Z axis→ 1	2	3	4	5	6	7	8	9	10
1	20.00	19.47	18.95	18.42	17.89	17.37	16.84	16.32	15.79	15.26
2	18.92	18.73	18.40	18.00	17.57	17.12	16.66	16.19	15.71	15.24
3	18.22	18.13	17.91	17.61	17.26	16.88	16.48	16.06	15.64	15.21
4	17.71	17.66	17.50	17.27	16.98	16.66	16.31	15.95	15.57	15.19
5	17.32	17.28	17.16	16.98	16.74	16.47	16.17	15.85	15.51	15.17
6	17.02	16.99	16.89	16.74	16.54	16.30	16.04	15.76	15.46	15.15
7	16.78	16.75	16.67	16.54	16.37	16.17	15.93	15.68	15.41	15.14
8	16.60	16.57	16.50	16.39	16.24	16.06	15.85	15.62	15.38	15.13
9	16.46	16.44	16.38	16.28	16.14	15.97	15.78	15.57	15.35	15.12
10	16.37	16.35	16.29	16.20	16.07	15.92	15.74	15.54	15.33	15.11
11	16.31	16.29	16.24	16.15	16.03	15.88	15.71	15.52	15.32	15.11
12	16.29	16.28	16.22	16.13	16.02	15.87	15.70	15.51	15.31	15.11

Y axis ↓	Z axis → 11	12	13	14	15	16	17	18	19	20
1	14.74	14.21	13.68	13.16	12.63	12.11	11.58	11.05	10.53	10.00
2	14.76	14.29	13.81	13.34	12.88	12.43	12.00	11.60	11.27	11.08
3	14.79	14.36	13.94	13.52	13.12	12.74	12.39	12.09	11.87	11.78
4	14.81	14.43	14.05	13.69	13.34	13.02	12.73	12.50	12.34	12.29
5	14.83	14.49	14.15	13.83	13.53	13.26	13.02	12.84	12.72	12.68
6	14.85	14.54	14.24	13.96	13.70	13.46	13.26	13.11	13.01	12.98
7	14.86	14.59	14.32	14.07	13.83	13.63	13.46	13.33	13.25	13.22
8	14.87	14.62	14.38	14.15	13.94	13.76	13.61	13.50	13.43	13.40
9	14.88	14.65	14.43	14.22	14.03	13.86	13.72	13.62	13.56	13.54
10	14.89	14.67	14.46	14.26	14.08	13.93	13.80	13.71	13.65	13.63
11	14.89	14.68	14.48	14.29	14.12	13.97	13.85	13.76	13.71	13.69
12	14.89	14.69	14.49	14.30	14.13	13.98	13.87	13.78	13.72	13.71

APPENDIX B

Correction Matrices

Table 4

Correction Matrix for an Upper and Lower Hydraulic Conductivity Equal to 1.0

Y axis ↓	Z axis → 1	2	3	4	5	6	7	8	9	10
1	0	0	0	0	0	0	0	0	0	0
2	-.086	-.082	-.075	-.066	-.056	-.046	-.036	-.026	-.016	-.005
3	-.102	-.009	-.092	-.082	-.071	-.059	-.046	-.033	-.020	-.007
4	-.009	-.097	-.091	-.082	-.072	-.060	-.047	-.034	-.021	-.007
5	-.092	-.090	-.085	-.078	-.069	-.058	-.046	-.033	-.020	-.007
6	-.084	-.084	-.079	-.072	-.064	-.054	-.043	-.031	-.019	-.006
7	-.077	-.076	-.072	-.067	-.059	-.050	-.040	-.029	-.018	-.006
8	-.071	-.070	-.067	-.062	-.055	-.047	-.038	-.027	-.017	-.006
9	-.066	-.065	-.062	-.058	-.051	-.044	-.035	-.026	-.016	-.005
10	-.063	-.062	-.059	-.055	-.049	-.042	-.034	-.025	-.015	-.005
11	-.060	-.060	-.057	-.053	-.047	-.041	-.033	-.024	-.015	-.005
12	-.060	-.059	-.056	-.052	-.047	-.040	-.032	-.024	-.014	-.005

Y axis ↓	Z axis → 11	12	13	14	15	16	17	18	19	20
1	0	0	0	0	0	0	0	0	0	0
2	.005	.015	.026	.036	.046	.056	.066	.075	.082	.086
3	.007	.020	.033	.046	.059	.071	.082	.092	.099	.102
4	.007	.021	.034	.048	.060	.072	.082	.091	.097	.099
5	.007	.020	.033	.046	.058	.069	.078	.085	.090	.092
6	.006	.019	.031	.043	.054	.064	.072	.079	.083	.084
7	.006	.018	.029	.040	.050	.059	.067	.072	.076	.077
8	.006	.017	.027	.038	.047	.055	.062	.067	.070	.071
9	.005	.016	.026	.035	.044	.051	.058	.062	.065	.066
10	.005	.015	.025	.034	.042	.049	.055	.059	.062	.063
11	.005	.015	.024	.033	.041	.047	.053	.057	.060	.060
12	.005	.014	.024	.032	.040	.047	.052	.056	.059	.060

Table 5

Correction Matrix for Upper Hydraulic Conductivity Equal to 1.0 and Lower Hydraulic Conductivity Equal to 100.0

Y axis ↓	Z axis → 1	2	3	4	5	6	7	8	9	10
1	0	0	0	0	0	0	0	0	0	0
2	-.080	-.076	-.069	-.060	-.051	-.042	-.033	-.023	-.014	-.005
3	-.082	-.080	-.073	-.065	-.056	-.046	-.036	-.026	-.015	-.005
4	-.064	-.063	-.058	-.052	-.045	-.037	-.029	-.021	-.013	-.004
5	-.041	-.040	-.037	-.034	-.029	-.024	-.019	-.014	-.008	-.003
6	-.016	-.015	-.014	-.013	-.011	-.009	-.007	-.005	-.003	-.001
7	-.003	-.002	-.002	-.002	-.002	-.002	-.001	-.001	-.001	-.000
8	-.002	-.002	-.002	-.002	-.002	-.002	-.001	-.001	-.001	-.000
9	-.002	-.002	-.002	-.002	-.002	-.001	-.001	-.001	-.001	-.000
10	-.002	-.002	-.002	-.002	-.002	-.001	-.001	-.001	-.001	-.000
11	-.002	-.002	-.002	-.002	-.002	-.001	-.001	-.001	-.000	-.000
12	-.002	-.002	-.002	-.002	-.002	-.001	-.001	-.001	-.000	-.000

Y axis ↓	Z axis → 11	12	13	14	15	16	17	18	19	20
1	0	0	0	0	0	0	0	0	0	0
2	.005	.014	.023	.033	.042	.051	.060	.069	.076	.080
3	.005	.015	.026	.036	.046	.056	.065	.073	.080	.082
4	.004	.013	.021	.029	.037	.045	.052	.058	.063	.064
5	.003	.008	.014	.019	.024	.029	.034	.037	.040	.041
6	.001	.003	.005	.007	.009	.011	.013	.014	.015	.016
7	.000	.001	.001	.001	.002	.002	.002	.002	.002	.003
8	.000	.001	.001	.001	.002	.002	.002	.002	.002	.002
9	.000	.001	.001	.001	.001	.002	.002	.002	.002	.002
10	.000	.001	.001	.001	.001	.002	.002	.002	.002	.002
11	.000	.000	.001	.001	.001	.002	.002	.002	.002	.002
12	.000	.000	.001	.001	.001	.002	.002	.002	.002	.002

Table 6

Correction Matrix for Upper Hydraulic Conductivity Equal to 100.0 and Lower Hydraulic Conductivity Equal to 1.0

Y axis ↓	Z axis → 1	2	3	4	5	6	7	8	9	10
1	0	0	0	0	0	0	0	0	0	0
2	-.086	-.082	-.075	-.066	-.056	-.046	-.036	-.026	-.015	-.005
3	-.106	-.103	-.096	-.086	-.074	-.062	-.048	-.035	-.021	-.007
4	-.110	-.108	-.101	-.092	-.080	-.067	-.053	-.038	-.023	-.007
5	-.110	-.108	-.102	-.093	-.082	-.069	-.055	-.039	-.024	-.008
6	-.109	-.108	-.102	-.093	-.082	-.070	-.056	-.040	-.025	-.008
7	-.105	-.103	-.098	-.090	-.080	-.067	-.054	-.039	-.024	-.008
8	-.097	-.096	-.091	-.084	-.075	-.064	-.051	-.037	-.023	-.007
9	-.091	-.090	-.086	-.079	-.071	-.060	-.048	-.035	-.022	-.007
10	-.087	-.085	-.082	-.076	-.068	-.058	-.046	-.034	-.021	-.007
11	-.084	-.083	-.079	-.074	-.066	-.057	-.046	-.034	-.021	-.006
12	-.083	-.082	-.078	-.073	-.065	-.056	-.045	-.033	-.020	-.006

Y axis ↓	Z axis → 11	12	13	14	15	16	17	18	19	20
1	0	0	0	0	0	0	0	0	0	0
2	.005	.015	.026	.036	.046	.057	.066	.075	.083	.086
3	.007	.021	.035	.048	.062	.074	.086	.096	.103	.106
4	.007	.023	.038	.053	.067	.080	.092	.101	.108	.110
5	.008	.024	.038	.055	.069	.082	.093	.102	.108	.110
6	.008	.025	.040	.056	.070	.082	.093	.103	.108	.109
7	.008	.024	.039	.054	.067	.080	.090	.098	.103	.105
8	.008	.023	.037	.051	.064	.075	.084	.091	.096	.097
9	.008	.022	.036	.048	.060	.071	.070	.086	.090	.091
10	.007	.021	.034	.046	.058	.068	.076	.082	.085	.087
11	.007	.021	.034	.046	.057	.066	.074	.079	.083	.084
12	.007	.020	.033	.045	.056	.065	.073	.078	.082	.083

APPENDIX C

Groundwater Potential Model

Table 7

Corrected Head Distribution in the Pahute Mesa-Yucca Flat Groundwater Model, Data in Meters

Y axis ↓	Z axis → 1	2	3	4	5	6	7	8	9	10
1	1445.	1440.	1439.	1430.	1421.	1419.	1415.	1412.	1408.	1405.
2	1345.	1344.	1345.	1343.	1341.	1339.	1336.	1339.	1338.	1339.
3	1336.	1336.	1336.	1333.	1331.	1328.	1325.	1328.	1327.	1328.
4	1341.	1342.	1342.	1337.	1334.	1333.	1329.	1331.	1329.	1329.
5	1350.	1350.	1350.	1347.	1344.	1343.	1340.	1342.	1339.	1338.
6	1360.	1359.	1358.	1357.	1355.	1355.	1352.	1353.	1349.	1346.
7	1365.	1365.	1364.	1362.	1360.	1360.	1357.	1357.	1354.	1350.

Y axis ↓	Z axis → 11	12	13	14	15	16	17	18	19	20
1	1400.	1395.	1380.	1370.	1360.	1355.	1340.	1330.	1325.	1320.
2	1342.	1337.	1335.	1325.	1321.	1317.	1308.	1311.	1289.	1278.
3	1328.	1320.	1324.	1313.	1311.	1306.	1297.	1297.	1279.	1270.
4	1329.	1320.	1323.	1312.	1310.	1304.	1294.	1293.	1276.	1270.
5	1337.	1327.	1329.	1318.	1314.	1308.	1297.	1294.	1278.	1273.
6	1344.	1335.	1335.	1324.	1320.	1313.	1302.	1298.	1282.	1277.
7	1348.	1339.	1339.	1328.	1323.	1315.	1304.	1301.	1285.	1279.

Y axis ↓	Z axis → 21	22	23	24	25	26	27	28	29	30
1	1300.	1280.	1260.	1245.	1221.	1200.	1180.	1160.	1140.	1120.
2	1272.	1268.	1256.	1245.	1245.	1226.	1214.	1202.	1184.	1179.
3	1252.	1252.	1257.	1245.	1247.	1230.	1224.	1215.	1184.	1068.
4	1253.	1251.	1249.	1242.	1249.	1235.	1220.	1110.	1028.	926.
5	1257.	1255.	1254.	1245.	1244.	1138.	1073.	986.	904.	844.
6	1263.	1252.	1230.	1131.	1082.	1007.	943.	853.	766.	771.
7	1265.	1252.								

Table 7 (cont'd)

Y axis ↓ / Z axis →	31	32	33	34	35	36	37	38	39	40
1	1100.	1075.	1050.	1020.	1000.	975.	950.	920.	900.	870.
2	1147.	1021.	903.	847.	809.	720.	737.	748.	745.	737.
3	966.	897.	843.	778.	780.	697.	703.	708.	708.	705.
4	755.	763.	766.	770.	774.	683.	680.	678.	677.	676.
5	759.	768.	769.	771.	772.	670.	658.	654.	652.	651.
6	763.	769.	769.	766.	759.	661.	627.	627.	627.	627.

Y axis ↓ / Z axis →	41	42	43	44	45	46	47	48
1	840.	820.	800.	780.	765.	755.	740.	720.
2	718.	711.	719.	716.	725.	707.	704.	704.
3	696.	690.	684.	687.	695.	679.	682.	686.
4	673.	669.	667.	669.	673.	654.	659.	660.
5	650.	648.	648.	648.	650.	627.	627.	627.
6	627.	627.	627.	627.	627.			

APPENDIX D

Computer Model Programs

```
      PROGRAM THESIS(INPUT,TAPE1=INPUT,OUTPUT,TAPE2=OUTPUT,PUNCH,TAPE3=P
     XUNCH)
      REAL BOX(12,21,20),MAT(12,20),ACCUM(240)
      REAL MATCOR(12,20),BOXCOR(12,20)
      REAL ACCUMB(20),ACCUMM(20),CORRFT(20),CORRMAT(12,20),KURT
      REAL LOWERK
      REAL CORRMOD(12,48),CORRFLP(7,48)
C*****************************************************************
C* THIS PROGRAM COMPUTES THE VALUES OF HEAD USING A THREE DIMENSIONAL. *
C*    AND A TWO DIMENSIONAL FINITE DIFFERENCE ALGORITHEM. THEN THE     *
C*    DIFFERENCE BETWEEN THE TWO SOLUTIONS IS STATISTICALY ANALYZED    *
C*    AND A CORRECTION FACTOR IS GENERATED.                            *
C*****************************************************************
C     BOX= THE THREE DEMENSIONAL MATRIX
C     MAT=THE TWO DEMENSOINAL MATRIX
C     UPPERK=THE HYDRAULIC CONDUCTIVITY FOR THE UPPER PART OF BOTH BOX
C            AND MAT
C     LOWERK=THE HYDRAULIC CONDUCTIVITY FOR THE LOWER PART OF BOTH BOX
C            AND MAT
C     HARMEAN= THE HYDRAULIC CONDUCTIVITY FOR THE SPACE BETWEEN THE
C              NODES IN THE UPPER HALF AND THE NODES IN THE LOWER HALF
C              OF THE MATRIX
C     CORRMAT=THE CORRECTION FACTOR
C     CORRMOD=THE CORRECTION FACTOR ALTERED TO FIT THE SIZE OF THE
C             GROUND WATER MODEL OF PAHUTE MESA TO YUCCA FLAT
C     CONMAX=THE MAXIMUM AMOUNT OF CHANGE AT CONVERGENCE
C     CONMIN=THE MINIMUN AMOUNT OF CHANGE AT CONVERGENCE
C     THE FOLLOWING SECTION IS SETUP
C*****************************************************************
      DO 3 I=1,12
      DO 3 J=1,21
      DO 3 K=1,20
    3 BOX(I,J,K)=15.0
      BOX(1,11,1)=20.0
      BOX(12,11,20)=10.0
      DO 6 K=1,14
```

```
    6   BOX(1,11,K+1)=(20.0-(0.526315789*K))
        DO 7 K=15,18
    7   BOX(12,11,K+1)=(20.0-(0.526315789*K))
        UPPERK=4.864
        LOWERK=1.0
        HARMEAN=(2.0*UPPERK*LOWERK)/(LOWERK+UPPERK)
        DENU=((5.0*UPPERK)+HARMEAN)
        DENL=((5.0*LOWERK)+HARMEAN)
        CONMAX=0.0000005
        CONMIN=-0.0000005
        DO 99 LLL=1,500
        XX=BOX(6,11,10)
C       THE FOLLOWING SECTION PERFORMES THE FINITE DIFFERENCE CALCULATIONS
C       THE FOLLOWING SECTION COMPUTES THE CORNERS
        BOX(1,1,1)=((BOX(2,1,1)*2.0)+(BOX(1,2,1)*2.0)+(BOX(1,1,2)*2.0))/6.
       X0
        BOX(1,21,1)=((BOX(2,21,1)*2.0)+(BOX(1,20,1)*2.0)+(BOX(1,21,2)*2.0)
       X)/6.0
        BOX(1,1,20)=((BOX(2,1,20)*2.0)+(BOX(1,2,20)*2.0)+(BOX(1,1,19)*2.0)
       X)/6.0
        BOX(1,21,20)=((BOX(2,21,20)*2.0)+(BOX(1,20,20)*2.0)+(BOX(1,21,19)*
       X2.0))/6.0
        BOX(12,1,1)=((BOX(11,1,1)*2.0)+(BOX(12,2,1)*2.0)+(BOX(12,1,2)*2.0)
       X)/6.0
        BOX(12,21,1)=((BOX(11,21,1)*2.0)+(BOX(12,20,1)*2.0)+(BOX(12,21,2)*
       X2.0))/6.0
        BOX(12,1,20)=((BOX(11,1,20)*2.0)+(BOX(12,2,20)*2.0)+(BOX(12,1,19)*
       X2.0))/6.0
        BOX(12,21,20)=((BOX(11,21,20)*2.0)+(BOX(12,20,20)*2.0)+(BOX(12,21,
       X19)*2.0))/6.0
C       THE FOLLOWING SECTION COMPUTES THE I EDGES
        DO 21 I=2,11
        IF(I.EQ.6) GO TO 22
        IF(I.EQ.7) GO TO 23
        BOX(I,1,1)=((BOX(I,2,1)*2.0)+(BOX(I,1,2)*2.0)+BOX(I+1,1,1)+BOX(I-1
       X,1,1))/6.0
```

```
      BOX(13-I,1,1)=((BOX(13-I,2,1)*2.0)+(BOX(13-I,1,2)*2.0)+BOX(13-I+1.
     X1,1)+BOX(13-I-1,1,1))/6.0
      BOX(I,1,20)=((BOX(I,2,20)*2.0)+(BOX(I,1,19)*2.0)+BOX(I+1,1.20)+BOX
     X(I-1,1,20))/6.0
      BOX(13-I,1,20)=((BOX(13-I,2,20)*2.0)+(BOX(13-I,1,19)*2.0)+BOX(13-I
     X+1,1.20)+BOX(13-I-1,1,20))/6.0
      BOX(I,21,1)=((BOX(I,20,1)*2.0)+(BOX(I,21,2)*2.0)+BOX(I+1,21.1)+BOX
     X(I-1,21,1))/6.0
      BOX(13-I,21,1)=((BOX(13-I,20,1)*2.0)+(BOX(13-I,21,2)*2.0)+BOX(13-I
     X+1,21,1)+BOX(13-I-1,21,1))/6.0
      BOX(I,21.20)=((BOX(I,20,20)*2.0)+(BOX(I,21,19)*2.0)+BOX(I+1.21.20)
     X+BOX(I-1,21,20))/6.0
      BOX(13-I,21,20)=((BOX(13-I,20,20)*2.0)+(BOX(13-I,21,19)*2.0)+BOX(1
     X3-I+1,21,20)+BOX(13-I-1,21,20))/6.0
      GO TO 21
   22 BOX(6,1,1)=((BOX(6,2,1)*2.0*UPPERK)+(BOX(6,1,2)*2.0*UPPERK)+(BOX(7
     X,1,1)*HARMEAN)+(BOX(5,1,1)*UPPERK))/((5.0*UPPERK)+HARMEAN)
      BOX(6,1,20)=((BOX(6,2,20)*2.0*UPPERK)+(BOX(6,1,19)*2.0*UPPERK)+(BO
     XX(7,1,20)*HARMEAN)+(BOX(5,1,20)*UPPERK))/((5.0*UPPERK)+HARMEAN)
      BOX(6,21,1)=((BOX(6,20,1)*2.0*UPPERK)+(BOX(6,21,2)*2.0*UPPERK)+(BO
     XX(7,21,1)*HARMEAN)+(BOX(5,21,1)*UPPERK))/((5.0*UPPERK)+HARMEAN)
      BOX(6,21,20)=((BOX(6,20,20)*2.0*UPPERK)+(BOX(6,21,19)*2.0*UPPERK)+
     X(BOX(7,21,20)*HARMEAN)+(BOX(5,21,20)*UPPERK))/((5.0*UPPERK)+HARMEA
     XN)
      GO TO 21
   23 BOX(7,1,1)=((BOX(7,2,1)*2.0*LOWERK)+(BOX(7,1,2)*2.0*LOWERK)+(BOX(8
     X,1,1)*LOWERK)+(BOX(6,1,1)*HARMEAN))/((5.0*LOWERK)+HARMEAN)
      BOX(7,1,20)=((BOX(7,2,20)*2.0*LOWERK)+(BOX(7,1,19)*2.0*LOWERK)+(BO
     XX(8,1,20)*LOWERK)+(BOX(6,1,20)*HARMEAN))/((5.0*LOWERK)+HARMEAN)
      BOX(7,21,1)=((BOX(7,20,1)*2.0*LOWERK)+(BOX(7,21,2)*2.0*LOWERK)+(BO
     XX(8,21,1)*LOWERK)+(BOX(6,21,1)*HARMEAN))/((5.0*LOWERK)+HARMEAN)
      BOX(7,21,20)=((BOX(7,20,20)*2.0*LOWERK)+(BOX(7,21,19)*2.0*LOWERK)+
     X(BOX(8,21,20)*LOWERK)+(BOX(6,21,20)*HARMEAN))/((5.0*LOWERK)+HARMEA
     XN)
   21 CONTINUE
C     THE FOLLOWING SECTION COMPUTES THE J EDGES
```

```
      DO 24 J=2,20
      BOX(1,J,20)=((BOX(2,J,20)*2.0)+(BOX(1,J,19)*2.0)+BOX(1,J+1,20)+BOX
     X(1,J-1,20))/6.0
      BOX(1,22-J,20)=((BOX(2,22-J,20)*2.0)+(BOX(1,22-J,19)*2.0)+BOX(1,22
     X-J+1,20)+BOX(1,22-J-1,20))/6.0
      IF(J.EQ.11) GO TO 15
      BOX(1,J,1)=((BOX(2,J,1)*2.0)+(BOX(1,J,2)*2.0)+BOX(1,J+1,1)+BOX(1,J
     X-1,1))/6.0
      BOX(1,22-J,1)=((BOX(2,22-J,1)*2.0)+(BOX(1,22-J,2)*2.0)+BOX(1,22-J+
     X1,1)+BOX(1,22-J-1,1))/6.0
   15 BOX(12,J,1)=((BOX(11,J,1)*2.0)+(BOX(12,J,2)*2.0)+BOX(12,J+1,1)+BOX
     X(12,J-1,1))/6.0
      BOX(12,22-J,1)=((BOX(11,22-J,1)*2.0)+(BOX(12,22-J,2)*2.0)+BOX(12,2
     X2-J+1,1)+BOX(12,22-J-1,1))/6.0
      IF(J.EQ.11) GO TO 24
      BOX(12,22-J,20)=((BOX(11,22-J,20)*2.0)+(BOX(12,22-J,19)*2.0)+BOX(1
     X2,22-J+1,20)+BOX(12,22-J-1,20))/6.0
      BOX(12,J,20)=((BOX(11,J,20)*2.0)+(BOX(12,J,19)*2.0)+BOX(12,J+1,20)
     X+BOX(12,J-1,20))/6.0
   24 CONTINUE
C     THE FOLLOWING SECTION COMPUTES THE K EDGES
      DO 25 K=16,19
   25 BOX(1,11,K)=((BOX(2,11,K)*2.0)+BOX(1,12,K)+BOX(1,10,K)+BOX(1,11,K+
     X1)+BOX(1,11,K-1))/6.0
      DO 27 K=2,19
      BOX(1,1,K)=((BOX(2,1,K)*2.0)+(BOX(1,2,K)*2.0)+BOX(1,1,K+1)+BOX(1,1
     X,K-1))/6.0
      BOX(1,1,21-K)=((BOX(2,1,21-K)*2.0)+(BOX(1,2,21-K)*2.0)+BOX(1,1,21-
     XK+1)+BOX(1,1,21-K-1))/6.0
      BOX(1,21,K)=((BOX(2,21,K)*2.0)+(BOX(1,20,K)*2.0)+BOX(1,21,K+1)+BOX
     X(1,21,K-1))/6.0
      BOX(1,21,21-K)=((BOX(2,21,21-K)*2.0)+(BOX(1,20,21-K)*2.0)+BOX(1,21
     X,21-K+1)+BOX(1,21,21-K-1))/6.0
      BOX(12,1,K)=((BOX(11,1,K)*2.0)+(BOX(12,2,K)*2.0)+BOX(12,1,K+1)+BOX
     X(12,1,K-1))/6.0
      BOX(12,1,21-K)=((BOX(11,1,21-K)*2.0)+(BOX(12,2,21-K)*2.0)+BOX(12,1
```

```
     X,21-K+1)+BOX(12,1,21-K-1))/6.0
      BOX(12,21,21-K)=((BOX(11,21,21-K)*2.0)+(BOX(12,20,21-K)*2.0)+BOX(1
     X2,21,21-K+1)+BOX(12,21,21-K-1))/6.0
   27 BOX(12,21,K)=((BOX(11,21,K)*2.0)+(BOX(12,20,K)*2.0)+BOX(12.21.K+1)
     X+BOX(12,21,K-1))/6.0
C     THE FOLLOWING SECTION COMPUTES THE IJ SIDES
      DO 30 I=2,11
      DO 30 J=2,20
      IF(I.EQ.6) GO TO 28
      IF(I.EQ.7) GO TO 29
      BOX(I,J,1)=((BOX(I,J,2)*2.0)+BOX(I+1,J,1)+BOX(I-1,J,1)+BOX(I,J+1,1
     X)+BOX(I,J-1,1))/6.0
      BOX(13-I,22-J,1)=((BOX(13-I,22-J,2)*2.0)+BOX(13-I+1,22-J,1)+BOX(13
     X-I-1,22-J,1)+BOX(13-I,22-J+1,1)+BOX(13-I,22-J-1,1))/6.0
      BOX(I,J,20)=((BOX(I,J,19)*2.0)+BOX(I+1,J,20)+BOX(I-1,J,20)+BOX(I,J
     X+1,20)+BOX(I,J-1,20))/6.0
      BOX(13-I,22-J,20)=((BOX(13-I,22-J,19)*2.0)+BOX(13-I+1,22-J,20)+BOX
     X(13-I-1,22-J,20)+BOX(13-I,22-J+1,20)+BOX(13-I,22-J-1,20))/6.0
      GO TO 30
   28 BOX(6,J,1)=((BOX(6,J,2)*2.0*UPPERK)+(BOX(7,J,1)*HARMEAN)+(BOX(5.J.
     X1)*UPPERK)+(BOX(6,J+1,1)*UPPERK)+(BOX(6,J-1,1)*UPPERK))/((5.0*UPPE
     XRK)+HARMEAN)
      BOX(7,22-J,1)=((BOX(7,22-J,2)*2.0*LOWERK)+(BOX(8,22-J,1)*LOWERK)+(
     XBOX(6,22-J,1)*HARMEAN)+(BOX(7,22-J+1,1)*LOWERK)+(BOX(7,22-J-1.1)*L
     XOWERK))/((5.0*LOWERK)+HARMEAN)
      BOX(6,J,20)=((BOX(6,J,19)*2.0*UPPERK)+(BOX(7,J,20)*HARMEAN)+(BOX(5
     X,J,20)*UPPERK)+(BOX(6,J+1,20)*UPPERK)+(BOX(6,J-1,20)*UPPERK))/((5.
     X0*UPPERK)+HARMEAN)
      BOX(7,22-J,20)=((BOX(7,22-J,19)*2.0*LOWERK)+(BOX(8,22-J,20)*LOWERK
     X)+(BOX(6,22-J,20)*HARMEAN)+(BOX(7,22-J+1,20)*LOWERK)+(BOX(7.22-J-1
     X,20)*LOWERK))/((5.0*LOWERK)+HARMEAN)
      GO TO 30
   29 BOX(7,J,1)=((BOX(7,J,2)*2.0*LOWERK)+(BOX(8,J,1)*LOWERK)+(BOX(6,J,1
     X)*HARMEAN)+(BOX(7,J+1,1)*LOWERK)+(BOX(7,J-1,1)*LOWERK))/((5.0*LOWE
     XRK)+HARMEAN)
      BOX(6,22-J,1)=((BOX(6,22-J,2)*2.0*UPPERK)+(BOX(7,22-J,1)*HARMEAN)+
```

```
     X(BOX(5,22-J,1)*UPPERK)+(BOX(6,22-J+1,1)*UPPERK)+(BOX(6,22-J-1.1)*U
     XPPERK))/((5.0*UPPERK)+HARMEAN)
      BOX(7,J,20)=((BOX(7,J,19)*2.0*LOWERK)+(BOX(8,J,20)*LOWERK)+(BOX(6.
     XJ,20)*HARMEAN)+(BOX(7,J+1,20)*LOWERK)+(BOX(7,J-1,20)*LOWERK))/((5.
     X0*LOWERK)+HARMEAN)
      BOX(6,22-J,20)=((BOX(6,22-J,19)*2.0*UPPERK)+(BOX(7,22-J,20)*HARMEA
     XN)+(BOX(5,22-J,20)*UPPERK)+(BOX(6,22-J+1,20)*UPPERK)+(BOX(6,22-J-1
     X,20)*UPPERK))/((5.0*UPPERK)+HARMEAN)
   30 CONTINUE
C     THE FOLLOWING SECTION COMPUTES THE IK SIDES
      DO 33 I=2,11
      DO 33 K=2,19
      IF(I.EQ.6) GO TO 31
      IF(I.EQ.7) GO TO 32
      BOX(I,1,K)=((BOX(I,2,K)*2.0)+BOX(I+1,1,K)+BOX(I-1,1,K)+BOX(I,1,K+1
     X)+BOX(I,1,K-1))/6.0
      BOX(13-I,21,21-K)=((BOX(13-I,20,21-K)*2.0)+BOX(13-I+1,21,21-K)+BOX
     X(13-I-1,21,21-K)+BOX(13-I,21,21-K+1)+BOX(13-I,21,21-K-1))/6.0
      BOX(13-I,1,21-K)=((BOX(13-I,2,21-K)*2.0)+BOX(13-I+1,1,21-K)+BOX(13
     X-I-1,1,21-K)+BOX(13-I,1,21-K+1)+BOX(13-I,1,21-K-1))/6.0
      BOX(I,21,K)=((BOX(I,20,K)*2.0)+BOX(I+1,21,K)+BOX(I-1,21,K)+BOX(I,2
     X1,K+1)+BOX(I,21,K-1))/6.0
      GO TO 33
   31 BOX(6,1,K)=((BOX(6,2,K)*2.0*UPPERK)+(BOX(7,1,K)*HARMEAN)+(BOX(5.1,
     XK)*UPPERK)+(BOX(6,1,K+1)*UPPERK)+(BOX(6,1,K-1)*UPPERK))/((5.0*UPPE
     XRK)+HARMEAN)
      BOX(7,1,21-K)=((BOX(7,2,21-K)*2.0*LOWERK)+(BOX(8,1,21-K)*LOWERK)+(
     XBOX(6,1,21-K)*HARMEAN)+(BOX(7,1,21-K+1)*LOWERK)+(BOX(7,1,21-K-1)*L
     XOWERK))/((5.0*LOWERK)+HARMEAN)
      BOX(6,21,K)=((BOX(6,20,K)*2.0*UPPERK)+(BOX(7,21,K)*HARMEAN)+(BOX(5
     X,21,K)*UPPERK)+(BOX(6,21,K+1)*UPPERK)+(BOX(6,21,K-1)*UPPERK))/((5.
     X0*UPPERK)+HARMEAN)
      BOX(7,21,21-K)=((BOX(7,20,21-K)*2.0*LOWERK)+(BOX(8,21,21-K)*LOWERK
     X)+(BOX(6,21,21-K)*HARMEAN)+(BOX(7,21,21-K+1)*LOWERK)+(BOX(7,21,21-
     XK-1)*LOWERK))/((5.0*LOWERK)+HARMEAN)
      GO TO 33
```

```
   32  BOX(7,1,K)=((BOX(7,2,K)*2.0*LOWERK)+(BOX(8,1,K)*LOWERK)+(BOX(6.1,K
      X)*HARMEAN)+(BOX(7,1,K+1)*LOWERK)+(BOX(7,1,K-1)*LOWERK))/((5.0*LOWE
      XRK)+HARMEAN)
       BOX(6,1,21-K)=((BOX(6,2,21-K)*2.0*UPPERK)+(BOX(7,1,21-K)*HARMEAN)+
      X(BOX(5,1,21-K)*UPPERK)+(BOX(6,1,21-K+1)*UPPERK)+(BOX(6,1,21-K-1)*U
      XPPERK))/((5.0*UPPERK)+HARMEAN)
       BOX(7,21,K)=((BOX(7,20,K)*2.0*LOWERK)+(BOX(8,21,K)*LOWERK)+(BOX(6,
      X21,K)*HARMEAN)+(BOX(7,21,K+1)*LOWERK)+(BOX(7,21,K-1)*LOWERK))/((5.
      X0*LOWERK)+HARMEAN)
       BOX(5,21,21-K)=((BOX(6,20,21-K)*2.0*UPPERK)+(BOX(7,21,21-K)*HARMEA
      XN)+(BOX(5,21,21-K)*UPPERK)+(BOX(6,21,21-K+1)*UPPERK)+(BOX(6,21,21-
      XK-1)*UPPERK))/((5.0*UPPERK)+HARMEAN)
   33  CONTINUE
C      THE FOLLOWING SECTION COMPUTES THE JK SIDES
       DO 36 J=2,20
       DO 36 K=2,19
       IF(J.EQ.11.AND.K.LT.16)GO TO 36
       BOX(1,J,K)=((BOX(2,J,K)*2.0)+BOX(1,J+1,K)+BOX(1,J-1,K)+BOX(1,J,K+1
      X)+BOX(1,J,K-1))/6.0
   36  CONTINUE
       DO 35 K=2,19
       DO 35 J=2,20
       IF(J.EQ.11.AND.K.GT.15) GO TO 35
       BOX(12,J,K)=((BOX(11,J,K)*2.0)+BOX(12,J+1,K)+BOX(12,J-1,K)+BOX(12,
      XJ,K+1)+BOX(12,J,K-1))/6.0
   35  CONTINUE
C      THE FOLLOWING SECTION COMPUTES THE FINITE DIFFERENCE FOR THE
C      INTERIOR OF BOX
       DO 39 K=2,19
       DO 39 J=2,20
       DO 39 I=2,11
       IF(I.EQ.6) GO TO 37
       IF(I.EQ.7) GO TO 37
       BOX(I,J,K)=(BOX(I+1,J,K)+BOX(I-1,J,K)+BOX(I,J+1,K)+BOX(I,J-1,K)+BO
      XX(I,J,K+1)+BOX(I,J,K-1))/6.0
       BOX(13-I,22-J,21-K)=(BOX(13-I+1,22-J,21-K)+BOX(13-I-1,22-J,21-K)+B
```

```
     XOX(13-I,22-J+1,21-K)+BOX(13-I,22-J-1,21-K)+BOX(13-I,22-J,21-K+1)+B
     XOX(13-I,22-J,21-K-1))/6.0
      GO TO 39
   37 BOX(6,J,K)=((BOX(7,J,K)*HARMEAN)+((BOX(5,J,K)+BOX(6,J+1,K)+BOX(6,J
     X-1,K)+BOX(6,J,K+1)+BOX(6,J,K-1))*UPPERK))/DENU
      BOX(7,22-J,21-K)=((BOX(6,22-J,21-K)*HARMEAN)+((BOX(8,22-J,21-K)+BO
     XX(7,22-J+1,21-K)+BOX(7,22-J-1,21-K)+BOX(7,22-J,21-K+1)+BOX(7,22-J,
     X21-K-1))*LOWERK))/DENL
   39 CONTINUE
C     THE FOLLOWING SECTION IS A CONVERGENCE TEST AND A WRITE
      XX=BOX(6,11,10)-XX
      IF(XX.LT.CONMAX.AND.XX.GT.CONMIN) WRITE(2,50) LLL
   50 FORMAT(1H ,49H THE NUMBER OF ITERATIONS AT CONVERGENCE EQUALS  ,I3
     X)
      IF(XX.LT.CONMAX.AND.XX.GT.CONMIN) GO TO 88
   99 CONTINUE
C     THE FOLLOWING SECTION IS BOX-11 WRITE
   88 WRITE(2,51)
   51 FORMAT(1H-,34H THE AREA OF BOX EQUIVALENT TO MAT)
      DO 42 I=1,12
   42 WRITE(2,52)(BOX(I,11,K),K=1,20)
   52 FORMAT(1H ,20(1X,F5.2))
C     THE FOLLOWING SECTION PRINTS THE TOP AND BOTTOM SURFACES OF BOX
      WRITE (2,53)
   53 FORMAT(1H-,31H THE TOP SURFACE OF BOX EQUALS )
      WRITE(2,52)((BOX(1,J,K),K=1,20),J=1,21)
      WRITE(2,54)
   54 FORMAT(1H-,34H THE BOTTOM SURFACE OF BOX EQUALS )
      WRITE(2,52)((BOX(12,J,K),K=1,20),J=1,21)
C*****************************************************************
C* THIS PROGRAM SOLVES THE PARTIAL DIFFERENTIAL EQUATION FOR POTENTIAL *
C*   AS A TWO   DEMENSIONAL FINITE DIFFERENCE ALGORITHM              *
C*****************************************************************
C     THE FOLLOWING SECTION IS SETUP
      DU=((3.0*UPPERK)+HARMEAN)
      DL=((3.0*LOWERK)+HARMEAN)
```

```
      DO 103 I=1,12
      DO 103 K=1,20
 103  MAT(I,K)=15.0
      MAT(1,1)=20.0
      MAT(12,20)=10.0
      DO 109 K=1,14
 109  MAT(1,K+1)=(20.0-(0.526315789*K))
      DO 110 K=15,18
 110  MAT(12,K+1)=(20.0-(0.526315789*K))
C     THE FOLLOWING SECTION IS THE FINITE-DIFERENCE SEQUENCE FOR MAT
      DO 199 LLL=1,500
      XX=MAT(5,8)
C     THE FOLLOWING SECTION COMPUTES THE CORNERS
      MAT(12,1)=((MAT(11,1)*2.0)+(MAT(12,2)*2.0))/4.0
      MAT(1,20)=((MAT(2,20)*2.0)+(MAT(1,19)*2.0))/4.0
C     THE FOLLOWING SECTION COMPUTES THE SIDES
C     FRONT
      DO 106 I=2,11
      IF(I.EQ.6) GO TO 107
      IF(I.EQ.7) GO TO 108
      MAT(I,1)=((MAT(I,2)*2.0)+MAT(I+1,1)+MAT(I-1,1))/4.0
      MAT(13-I,1)=((MAT(13-I,2)*2.0)+MAT(13-I+1,1)+MAT(13-I-1,1))/4.0
C     BACK
      MAT(I,20)=((MAT(I,19)*2.0)+MAT(I+1,20)+MAT(I-1,20))/4.0
      MAT(13-I,20)=((MAT(13-I,19)*2.0)+MAT(13-I+1,20)+MAT(13-I-1,20))/4.
     X0
      GO TO 106
 107  MAT(6,1)=((MAT(6,2)*2.0*UPPERK)+(MAT(5,1)*UPPERK)+(MAT(7,1)*HARMEA
     XN))/DU
      MAT(6,20)=((MAT(6,19)*2.0*UPPERK)+(MAT(5,20)*UPPERK)+(MAT(7,20)*HA
     XRMEAN))/DU
      GO TO 106
 108  MAT(7,1)=((MAT(7,2)*2.0*LOWERK)+(MAT(6,1)*HARMEAN)+(MAT(8,1)*LOWER
     XK))/DL
      MAT(7,20)=((MAT(7,19)*2.0*LOWERK)+(MAT(8,20)*LOWERK)+(MAT(6,20)*HA
     XRMEAN))/DL
```

```
 106  CONTINUE
C     THE FOLLOWING SECTICN COMPUTES THE BOTTOM
      DO 112 K=2,15
 112  MAT(12,K)=((MAT(11,K)*2.0)+MAT(12,K+1)+MAT(12,K-1))/4.0
      DO 113 K=16,19
 113  MAT(1,K)=((MAT(2,K)*2.0)+MAT(1,K+1)+MAT(1,K-1))/4.0
      DO 115 K=2,19
      DO 115 I=2,11
      IF(I.EQ.6) GO TO 116
      IF(I.EQ.7) GO TO 117
      MAT(I,K)=(MAT(I+1,K)+MAT(I-1,K)+MAT(I,K+1)+MAT(I,K-1))/4.0
      MAT(13-I,21-K)=(MAT(13-I+1,21-K)+MAT(13-I-1,21-K)+MAT(13-I,21-K+1)
     X+MAT(13-I,21-K-1))/4.0
 116  MAT(6,K)=((MAT(6,K-1)*UPPERK)+(MAT(6,K+1)*UPPERK)+(MAT(5,K)*UPPERK
     X)+(MAT(7,K)*HARMEAN))/DU
      MAT(7,21-K)=((MAT(7,21-K-1)*LOWERK)+(MAT(7,21-K+1)*LOWERK)+(MAT(8,
     X21-K)*LCWERK)+(MAT(6,21-K)*HARMEAN))/DL
      GO TO 115
 117  MAT(7,K)=((MAT(7,K-1)*LOWERK)+(MAT(7,K+1)*LCWERK)+(MAT(8,K)*LOWERK
     X)+(MAT(6,K)*HARMEAN))/DL
      MAT(6,21-K)=((MAT(6,21-K-1)*UPPERK)+(MAT(6,21-K+1)*UPPERK)+(MAT(5,
     X21-K)*UPPERK)+(MAT(7,21-K)*HARMEAN))/DU
 115  CONTINUE
      XX=MAT(5,8)-XX
      IF(XX.LT.CONMAX.AND.XX.GT.CONMIN) WRITE(2,150) LLL
 150  FCRMAT(1H-,56H THE NUMBER OF ITERATIONS IN MAT AT CONVERGENCE EQUA
     XLS  ,I6)
      IF(XX.LT.CONMAX.AND.XX.GT.CONMIN) GO TO 188
 199  CONTINUE
C     THE FCLLOWING SECTION IS MAT WRITE
 188  WRITE(2,151)
 151  FCRMAT(1H-,22H THE MATRIX MAT EQUALS)
      DO 124 I=1,12
 124  WRITE(2,152)(MAT(I,K),K=1,20)
 152  FCRMAT(1H ,20(1X,F5.2))
C*********************************************************************
```

```
C*     THE FOLLOWING SECTION COMPUTES A CORRECTION FACTOR TO BE USED TO *
C*     SIMULATE THE THREE DEMENSIONAL FINITE DIFFERENCE ALGORITHUM WITH *
C*     A TWO DEMENSIONAL FINITE DIFFERENCE ALGORITHUM PLUS  THE         *
C*     CORRECTION FACTOR CALLED CORRFT                                  *
C*****************************************************************
C      ACCUMB=THE ACCUMULATOR FOR CALCULATIONS ON BOX
C      ACCUMM=THE ACCUMULATOR FOR CALCULATIONS ON MAT
       DO 203 K=1,20
       ACCUMB(K)=0.0
 203   ACCUMM(K)=0.0
       DO 206 I=1,12
       DO 206 K=1,20
       MATCOR(I,K)=MAT(I,K)/15.0
       BOXCOR(I,K)=BOX(I,11,K)/15.0
 206   CORRMAT(I,K)=BOXCOR(I,K)-MATCOR(I,K)
       WRITE(2,250)
 250   FORMAT(1H-,15H SECTION NUMBER,10X,12H BOX AVERAGE,10X,12H MAT AVER
      XAGE,10X,26H AVERAGE CORRECTION FACTOR)
       DO 209 K=1,20
       CORRFT(K)=0.0
       DO 212 I=1,12
       CORRFT(K)=CORRFT(K)+CORRMAT(I,K)
       ACCUMB(K)=BOX(I,11,K)+ACCUMB(K)
 212   ACCUMM(K)=MAT(I,K)+ACCUMM(K)
       ACCUMB(K)=ACCUMB(K)/12.0
       ACCUMM(K)=ACCUMM(K)/12.0
       CORRFT(K)=CORRFT(K)/12.0
 209   WRITE(2,251) K,ACCUMB(K),ACCUMM(K),CORRFT(K)
 251   FORMAT(1H ,6X,I2,23X,F7.4,16X,F7.4,21X,F7.5)
       WRITE(2,252)
 252   FORMAT(1H-,22H THE CORRECTION MATRIX)
       DO 218 I=1,12
       DO 218 K=1,20,5
 218   WRITE(2,253)CORRMAT(I,K),I,K,CORRMAT(I,K+1),I,K+1,CORRMAT(I,K+2),I
      X,K+2,CORRMAT(I,K+3),I,K+3,CORRMAT(I,K+4),I,K+4
 253   FORMAT(1H ,5(F10.7,1X,I3,1X,I3,3X))
```

```
      WRITE(2,252)
      DO 221 I=1,12
 221  WRITE(2,254)(CORRMAT(I,K),K=1,20)
 254  FORMAT(1H ,20(1X,F5.3))
C*****************************************************************
C*    THE FOLLOWING SECTION COMPARES THE THREE DEMENSIONALY DERIVED    *
C*    SOLUTION WITH THE TWO DIMENSIONALY DERIVED MAT AND PERFORM A     *
C*    NUMBER OF STATISTICAL TESTS ON THE DIFFERENCE BETWEEN THEM       *
C*****************************************************************
C     THE FOLLOWING SECTION SETS THE LIMITS TO WHICH THE PROGRAM WILL
C     FUNCTION   NUM=THE NUMBER OF OBSERVATIONS.
      NUM=220
      XNUM=220.0
      IX=0
      SUM=0.0
      WRITE(2,350)
 350  FORMAT(1H-,64H THE STATISTICAL RESULTS OF THE ENTIRE CORRECTION MA
     XTRIX EQUALS )
C     THE FOLLOWING SECTION CALCULATES AVERAGE
      DO 303  I=1,12
      DO 303 K=1,20
 303  SUM=SUM+CORRMAT(I,K)
      XBAR=SUM/XNUM
      WRITE(2,352)XBAR
 352  FORMAT(1H ,37H THE AVERAGE VALUE OF CORRMAT EQUALS ,F12.9)
      DO 306 I=2,12
      DO 306 K=1,20
      IX=IX+1
 306  ACCUM(IX)=CORRMAT(I,K)-XBAR
      K=0
      GO TO 399
 388  K=K+1
      WRITE(2,351) K
 351  FORMAT(1H-,34H THE STATISTICAL RESULT OF COLUMN ,I2,8H EQUALS )
      DO 318 I=2,12
 318  SUM=SUM+CORRMAT(I,K)
```

```
      XBAR=SUM/XNUM
      WRITE(2,352) XBAR
      DO 321 I=2,12
 321  ACCUM(I)=CORRMAT(I,K)-XBAR
 399  CONTINUE
      SUM=0.0
      DO 309 I=1,NUM
 309  SUM=SUM+(ACCUM(I)**2.0)
C     THE FOLLOWING SECTION CALCULATES VARIANCE
      VAR=SUM/(XNUM-1)
      WRITE(2,353) VAR
 353  FORMAT(1H ,32H THE VARIENCE OF CORRMAT EQUALS ,F12.9)
C     THE FOLLOWING SECTION CALCULATES STANDARD DEVIATION
      STDEV=VAR**0.5
      WRITE(2,354) STDEV
 354  FORMAT(1H ,42H THE STANDARD DEVIATION OF CORRMAT EQUALS ,F12.9)
      SUM=0.0
C     THE FOLLOWING SECTION CALCULATES SKEW
      DO 312  I=1,NUM
 312  SUM=SUM+(ACCUM(I)**3)
      SKEW=SUM/((XNUM-1)*(STDEV**3.0))
      WRITE(2,355) SKEW
 355  FORMAT(1H ,29H THE SKEW OF CORRMAT EQUALS ,F12.9)
C     THE FOLLOWING SECTION CALCULATES KURTOSIS
      SUM=0.0
      DO 315 I=1,NUM
 315  SUM=SUM+(ACCUM(I)**4.0)
      KURT=SUM/((XNUM-1)*(STDEV**4.0))
      WRITE(2,356) KURT
 356  FORMAT(1H ,32H THE KURTOSIS OF CORRMAT EQUALS ,F12.9)
      IX=0
      NUM=12
      XNUM=11.0
      IF(K.LT.20) GO TO 388
C*****************************************************************
C*    THE FOLLOWING PROGRAM ADJUSTS THE CORRECTION MATRIX TO FIT THE   *
```

```
C*     MODEL OF THE PAHUTE MESA - YUCCA FLAT GROUND WATER SYSTEM        *
C*********************************************************************
      DO 403 I=2,12
      L=0
      DO 403 K=1,48,12
      L=L+1
      CORRMOD(I,K)=CORRMAT(I,L)
      CORRMOD(I,K+1)=CORRMAT(I,L)
      CORRMOD(I,K+2)=(CORRMAT(I,L)*0.4166)+(CORRMAT(I,L+1)*0.5833)
      L=L+1
      CORRMOD(I,K+3)=CORRMAT(I,L)
      CORRMOD(I,K+4)=(CORRMAT(I,L)*0.8166)+(CORRMAT(I,L+1)*0.1833)
      L=L+1
      CORRMOD(I,K+5)=CORRMAT(I,L)
      CORRMOD(I,K+6)=CORRMAT(I,L)
      CORRMOD(I,K+7)=(CORRMAT(I,L)*0.2166)+(CORRMAT(I,L+1)*0.7833)
      L=L+1
      CORRMOD(I,K+8)=CORRMAT(I,L)
      CORRMOD(I,K+9)=(CORRMAT(I,L)*0.6166)+(CORRMAT(I,L+1)*0.3833)
      L=L+1
      CORRMOD(I,K+10)=CORRMAT(I,L)
 403  CORRMOD(I,K+11)=CORRMAT(I,L)
      DO 406 K=1,22
      CORRMOD(2,K)=(CORRMOD(2,K)+(CORRMOD(3,K)*0.8333))
      CORRMOD(3,K)=((CORRMOD(3,K)*0.1666)+CORRMOD(4,K)+(CORRMOD(5,K)*0.6
     X666))
      CORRMOD(4,K)=((CORRMOD(5,K)*0.3333)+CORRMOD(6,K)+(CORRMOD(7,K)*0.5
     X))
      CORRMOD(5,K)=((CORRMOD(7,K)*0.5)+CORRMOD(8,K)+(CORRMOD(9,K)*0.3333
     X))
      CORRMOD(6,K)=((CORRMOD(9,K)*0.6666)+CORRMOD(10,K)+(CORRMOD(11,K)*0
     X.1666))
 406  CORRMOD(7,K)=((CORRMOD(12,K)*0.8333)+CORRMOD(12,K))
      DO 409 K=23,36
      CORRMOD(3,K)=(CORRMOD(2,K)+CORRMOD(3,K)+(CORRMOD(4,K)*0.2))
      CORRMOD(4,K)=((CORRMOD(4,K)*0.8)+CORRMOD(5,K)+(CORRMOD(6,K)*0.4))
```

```
      CORRMOD(5,K)=((CORRMOD(6,K)*0.6)+CORRMOD(7,K)+(CORRMOD(8,K)*0.6))
      CORRMOD(6,K)=((CORRMOD(8,K)*0.4)+CORRMOD(9,K)+(CORRMOD(10,K)*0.8))
409   CORRMOD(7,K)=((CORRMOD(10,K)*0.2)+CORRMOD(11,K)+CORRMOD(12,K))
      DO 412 K=37,45
      TEMPONE=(CORRMOD(1,K)+CORRMOD(2,K)+(CORRMOD(3,K)*0.75))
      TEMPTWO=((CORRMOD(3,K)*0.25)+CORRMOD(4,K)+CORRMOD(5,K)+(CORRMOD(6,
     XK)*0.5))
      CORRMOD(3,K)=TEMPONE
      CORRMOD(4,K)=TEMPTWO
      CORRMOD(5,K)=((CORRMOD(6,K)*0.5)+CORRMOD(7,K)+CORRMOD(8,K)+(CORRMO
     XD(09,K)*0.25))
412   CORRMOD(6,K)=((CORRMOD(09,K)*0.75)+CORRMOD(10,K)+CORRMOD(11,K))
      DO 413 K=46,47
      TEMPONE=(CORRMOD(1,K)+CORRMOD(2,K)+CORRMOD(3,K)+(CORRMOD(4,K)*0.66
     X66))*(3.0/11.0)
      TEMPTWO=((CORRMOD(4,K)*0.3333)+CORRMOD(5,K)+CORRMOD(6,K)+CORRMOD(7
     X,K)+(CORRMOD(8,K)*0.3333))*(3.0/11.0)
      TEMPTHR=((CORRMOD(8,K)*0.6666)+CORRMOD(09,K)+CORRMOD(10,K)+CORRMOD
     X(11,K))*(3.0/11.0)
      CORRMOD(4,K)=TEMPONE
      CORRMOD(5,K)=TEMPTWO
413   CORRMOD(6,K)=TEMPTHR
      DO 423 I=2,7
      DO 423 K=1,22
423   CORRMOD(I,K)=CORRMOD(I,K)*(6.0/11.0)
      DO 427 I=3,7
      DO 427 K=23,36
427   CORRMOD(I,K)=CORRMOD(I,K)*(5.0/11.0)
      DO 430 I=3,6
      DO 430 K=37,45
430   CORRMOD(I,K)=CORRMOD(I,K)*(4.0/11.0)
      WRITE(2,450)
450   FORMAT(1H-,63H THE FIRST PART OF THE CORRECTION MATRIX FOR THE PAH
     X-YUC MODEL )
      DO 415 I=2,7
415   WRITE(2,451)(CORRMOD(I,K),K=1,11)
```

```
451  FCRMAT(1H ,11(1X,F5.3))
     WRDT (2,456)
456  FCRMAT(1H-,5H      )
     DO 416 I=2,7
416  WRDTE(2,451)(CORRMOD(I,K),K=12,22)
     WRITE(2,452)
452  FORMAT(1H-,64H THE SECOND PART OF THE CORRECTION MATRIX FOR THE PA
    XH-YUC MCDEL )
     DO 418 I=3,7
418  WRITE(2,451)(CORRMOD(I,K),K=23,33)
     WRITE(2,456)
     DC 419 I=3,7
419  WRDTE(2,454)(CORRMOC(I,K),K=34,45)
454  FCRMAT(1H ,12(1X,F5.3))
     WRITE(2,453)
453  FCRMAT(1H-,63H THE THIRD PART OF THE CORRECTION MATRIX FOR THE PAH
    X-YUC MODEL )
     DO 421 I=4,7
421  WRITE(2,455)(CORRMOC(I,K),K=46,48)
455  FCRMAT(1H ,3(1X,F5.3))
     DO 440 K=1,22
440  WRDTE(3,459)(CORRMOD(I,K),I=2,7)
459  FORMAT(1H ,6(F7.4,3X))
     DO 442 K=23,45
442  WRITE(3,457)(CORRMOC(I,K),I=3,7)
457  FORMAT(1H ,5(F7.4,3X))
     DO 445 K=46,48
445  WRITE(3,458)(CORRMOD(I,K),I=4,7)
458  FCRMAT(1H ,4(F7.4,3X))
```

```
      PROGRAM PAHYUC(INPUT,TAPE1=INPUT,OUTPUT,TAPE2=OUTPUT)
      REAL HYDCON(7,48),CORRMAT(7,48),PYMOD(7,48)
      REAL LOWERK
      REAL PYCORR(7,48)
      DO 1 I=1,7
      DO 1 K=1,48
    1 PYMOD(I,K)=1082.5
      DO 3 K=1,22
    3 READ(1,50)(HYDCON(I,K),I=1,7)
   50 FORMAT(7(F10.6))
      DO 6 K=23,45
    6 READ(1,51)(HYDCON(I,K),I=2,7)
   51 FORMAT(6(F10.6))
      DO 9 K=46,48
    9 READ(1,52)(HYDCON(I,K),I=3,7)
   52 FORMAT(5(F10.6))
      DO 12 K=1,22
   12 READ(1,53)(CORRMAT(I,K),I=2,7)
   53 FORMAT(1X,6(F7.4,3X))
      DO 15 K=23,45
   15 READ(1,54)(CORRMAT(I,K),I=3,7)
   54 FORMAT(1X,5(F7.4,3X))
      DO 18 K=46,48
   18 READ(1,55)(CORRMAT(I,K),I=4,7)
   55 FORMAT(1X,4(F7.4,3X))
      DO 21 K=1,22,6
   21 READ(1,56)(PYMOD(1,L),L=K,K+5)
   56 FORMAT(6(F4.0,2X))
      DO 24 K=23,45,6
   24 READ(1,57)(PYMOD(2,L),L=K,K+5)
   57 FORMAT(6(F4.0,2X))
      READ(1,58)(PYMOD(3,L),L=46,48)
   58 FORMAT(3(F4.0,2X))
C     THE FOLLOWING SECTION COMPUTES THE FINITE DIFFERENCE EQUATIONS
      DO 99 LLL=1,10000
      XX=PYMOD(4,24)
```

```
C     THE FOLLOWING SECTION COMPUTES THE CORNERS
      PYMOD(7,1)=((PYMOD(7,2)*2.0*HYDCON(7,1))+(PYMOD(6,1)*2.0*HYDCON(6,
     X1)))/((HYDCON(7,1)*2.0)+(HYDCON(6,1)*2.0))
C     THE FOLLOWING SECTION COMPUTES THE SIDES
      DO 30 I=2,6
   30 PYMOD(I,1)=((PYMOD(I,2)*2.0*HYDCON(I,1))+(PYMOD(I+1,1)*HYDCON(I+1,
     X1))+(PYMOD(I-1,1)*HYDCON(I,1)))/((HYDCON(I,1)*2.0)+HYDCON(I+1,1)+H
     XYDCON(I,1))
      DO 33 I=4,6
   33 PYMOD(I,48)=((PYMOD(I,47)*2.0*HYDCON(I,47))+(PYMOD(I+1,48)*HYDCON(
     XI+1,48))+(PYMOD(I-1,48)*HYDCON(I,48)))/((HYDCON(I,47)*2.0)+HYDCON(
     XI+1,48)+HYDCON(I,48))
      DO 36 K=2,36
   36 PYMOD(7,K)=((PYMOD(6,K)*2.0*HYDCON(6,K))+(PYMOD(7,K+1)*HYDCON(7,K)
     X)+(PYMOD(7,K-1)*HYDCON(7,K-1)))/((HYDCON(6,K)*2.0)+HYDCON(7,K-1)+H
     XYDCON(7,K))
      DO 37 K=37,48
   37 PYMOD(7,K)=627.0
      DO 39 I=2,6
      DO 39 K=2,22
   39 PYMOD(I,K)=((PYMOD(I+1,K)*HYDCON(I,K))+(PYMOD(I-1,K)*HYDCON(I-1,K)
     X)+(PYMOD(I,K+1)*HYDCON(I,K))+(PYMOD(I,K-1)*HYDCON(I,K-1)))/(HYDCON
     X(I,K)+HYDCON(I-1,K)+HYDCON(I,K)+HYDCON(I,K-1))
      DO 42 I=3,6
      DO 42 K=23,45
   42 PYMOD(I,K)=((PYMOD(I+1,K)*HYDCON(I,K))+(PYMOD(I-1,K)*HYDCON(I-1,K)
     X)+(PYMOD(I,K+1)*HYDCON(I,K))+(PYMOD(I,K-1)*HYDCON(I,K-1)))/(HYDCON
     X(I,K)+HYDCON(I-1,K)+HYDCON(I,K)+HYDCON(I,K-1))
      DO 45 I=4,6
      DO 45 K=46,47
   45 PYMOD(I,K)=((PYMOD(I+1,K)*HYDCON(I,K))+(PYMOD(I-1,K)*HYDCON(I-1,K)
     X)+(PYMOD(I,K+1)*HYDCON(I,K))+(PYMOD(I,K-1)*HYDCON(I,K-1)))/(HYDCON
     X(I,K)+HYDCON(I-1,K)+HYDCON(I,K)+HYDCON(I,K-1))
      XX=PYMOD(4,24)-XX
      IF(XX.LT.0.0001.AND.XX.GT.-0.0001)WRITE(2,59) LLL
   59 FORMAT(1H-,58H THE NUMBER OF ITERATIONS IN PYMOD AT CONVERGENCE EQ
```

```
     XUALS  ,I6)
      IF(XX.LT.0.0001.AND.XX.GT.-0.0001) GO TO 88
 99   CONTINUE
 88   WRITE(2,160)
160   FORMAT(1H-,70H THE HEAD DISTRIBUTION WITHIN THE PAHUTE MESA-YUCCA
     XFLAT MODEL EQUALS )
      WRITE(2,61)
 61   FORMAT(1H-,12H SECTION ONE)
      DO 48 I=1,7
 48   WRITE(2,62)(PYMOD(I,K),K=1,22)
 62   FORMAT(1H ,22(F5.0))
      WRITE(2,63)
 63   FORMAT(1H-,12H SECTION TWO)
      DO 49 I=2,7
 49   WRITE(2,64)(PYMOD(I,K),K=23,45)
 64   FORMAT(1H ,23(F5.0))
      WRITE(2,65)
 65   FORMAT(1H-,14H SECTION THREE)
      DO 73 I=3,7
 73   WRITE(2,66)(PYMOD(I,K),K=46,48)
 66   FORMAT(1H ,3(F5.0))
      WRITE(2,67)
 67   FORMAT(1H-,60H THE HYDRAULIC CONDUCTIVITY VALUES USED IN THE PAH-Y
     XUC MODEL)
      WRITE(2,61)
      DO 76 K=1,22
 76   WRITE(2,68)(HYDCON(I,K),I=1,7)
 68   FORMAT(1H ,7(F10.6,5X))
      WRITE(2,63)
      DO 79 K=23,45
 79   WRITE(2,69)(HYDCON(I,K),I=2,7)
 69   FORMAT(1H ,6(F10.6,5X))
      WRITE(2,65)
      DO 81 K=46,48
 81   WRITE(2,70)(HYDCON(I,K),I=3,7)
 70   FORMAT(1H ,5(F10.6,5X))
```

```
      WRITE(2,150)
150   FORMAT(1H-,23H THE CORRECTION MATRIX )
      WRITE(2,61)
      DO 103 K=1,22
103   WRITE(2,69)(CORRMAT(I,K),I=2,7)
      WRITE(2,63)
      DO 106 K=23,45
106   WRITE(2,70)(CORRMAT(I,K),I=3,7)
      WRITE(2,65)
      DO 109 K=46,48
109   WRITE(2,112)(CORRMAT(I,K),I=4,7)
112   FORMAT(1H ,4(F10.6,5X))
      PYSUM=0.0
      DO 84 I=1,7
      DO 84 K=1,22
 84   PYSUM=PYSUM+PYMOD(I,K)
      DO 85 I=2,7
      DO 85 K=23,45
 85   PYSUM=PYSUM+PYMOD(I,K)
      DO 86 I=3,7
      DO 86 K=46,48
 86   PYSUM=PYSUM+PYMOD(I,K)
      AVEPY=PYSUM/307.0
      WRITE(2,153) AVEPY
153   FORMAT(1H-,47H THE AVERAGE VALUE OF THE PAH-YUC MODEL EQUALS ,F8.2
     X)
      DO 87 I=2,7
      DO 87 K=1,22
 87   PYCORR(I,K)=PYMOD(I,K)+(CORRMAT(I,K)*AVEPY)
      DO 89 I=3,7
      DO 89 K=23,36
 89   PYCORR(I,K)=PYMOD(I,K)+(CORRMAT(I,K)*AVEPY)
      DO 94 I=3,6
      DO 94 K=37,45
 94   PYCORR(I,K)=PYMOD(I,K)+(CORRMAT(I,K)*AVEPY)
      DO 99 I=4,6
```

```
      DO 90 K=46,48
 90   PYCORR(I,K)=PYMOD(I,K)+(CORRMAT(I,K)*AVEPY)
      WRITE(2,154)
154   FORMAT(1H-,80H THE CORRECTED HEAD DISTRIBUTION IN THE PAHUTE MESA-
     XYUCCA FLAT GROUNDWATER MODEL)
      WRITE(2,61)
      DO 91 I=1,7
 91   WRITE(2,62)(PYCORR(I,K),K=1,22)
      WRITE(2,63)
      DO 92 I=2,7
 92   WRITE(2,64)(PYCORR(I,K),K=23,45)
      WRITE(2,65)
      DO 93 I=3,7
 93   WRITE(2,66)(PYCORR(I,K),K=46,48)
      UPPERK=0.0
      LOWERK=0.0
      DO 200 K=1,22
      UPPERK=UPPERK+HYDCON(1,K)+HYDCON(2,K)+HYDCON(3,K)+(HYDCON(4,K)/2.0
     X)
200   LOWERK=LOWERK+(HYDCON(4,K)/2.0)+HYDCON(5,K)+HYDCON(6,K)+HYDCON(7,K
     X)
      DO 210 K=23,45
      UPPERK=UPPERK+HYDCON(2,K)+HYDCON(3,K)+HYDCON(4,K)
210   LOWERK=LOWERK+HYDCON(5,K)+HYDCON(6,K)+HYDCON(7,K)
      DO 220 K=46,48
      UPPERK=UPPERK+HYDCON(3,K)+HYDCON(4,K)+(HYDCON(5,K)/2.0)
220   LOWERK=LOWERK+(HYDCON(5,K)/2.0)+HYDCON(6,K)+HYDCON(7,K)
      UPPERK=UPPERK/153.5
      LOWERK=LOWERK/153.5
      WRITE(2,230) UPPERK,LOWERK
230   FORMAT(1H-,14H UPPERK EQUALS,F10.6,20X,14H LOWERK EQUALS,F10.6)
      STOP
      END
```

Distribution

U.S. Department of Energy, Nevada Operations Office, Las Vegas, NV:

E. M. Douthett (2)
P. B. Dunaway (2)
M. E. Gates, c/o R. R. Loux
R. W. Newman
D. A. Nowack (2)

U.S. Department of Energy, Nevada Test Site Support Office, Mercury, NV:

J. H. Dryden

U.S. Department of Energy, Mercury, NV:

CETO Library

U.S. Department of Energy, Washington, DC:

H. Hollister (2)
J. K. Bratton (2)
J. L. Liverman
Office of Public Affairs
W. H. Pennington

U.S. Department of Energy, Technical Information Center, Oak Ridge, TN: 27

Defense Nuclear Agency:

Test Construction Division, FCTC/DNA (Attn: J.W. LaComb, Clifford Snow), Mercury, NV

Director (Attn: SPSS, Milton Peek, Eugene Sevin, T.E. Kennedy); SPTD, Washington, D.C.

C.E. Keller, FCTMC/DNA, Kirtland AFB, NM

Los Alamos Scientific Laboratory, Los Alamos, NM:

R. B. Brownlee	Library
E. A. Bryant	K. H. Olsen
R. H. Campbell	R. R. Sharp
L. S. Germain	E. J. Sowder
J. W. House	T. A. Weaver

Lawrence Livermore Laboratory, Livermore, CA:

N. W. Howard	L. D. Ramspott
D. L. Springer	Technical Information Library Division
John Toman	Jack Kahn

Lawrence Livermore Laboratory, Mercury, NV:

W. B. McKinnis

Sandia Laboratories, Albuquerque, NM:

J. W. Banister
C. E. Broyles
M. L. Merritt
W. C. Vollendorf
W. D. Weart

Sandia Laboratories, Mercury, NV:

R. D. Statler
Howard P. Stephens

Defense Advanced Research Projects Agency, Arlington, VA:

G. H. Heilmeier

Colorado School of Mines, Golden, CO:

Maurice Major

Desert Research Institute, Reno, NV:

P. R. Fenske

Environmental Protection Agency, Seattle, WA:

Attn: Water Division

Environmental Protection Agency, National Environmental Research Center, Las Vegas, NV:

G. B. Morgan

National Oceanic and Atmospheric Administration, Weather Service Nuclear Support Office, Las Vegas, NV:

H. F. Mueller

Fenix & Scisson, Inc.:

Jack Cross, Las Vegas
Grant Bruesch, Mercury, NV

Holmes & Narver, Inc.:

F. M. Drake, Las Vegas, NV
Resident Manager, Mercury, NV

U. S. Army Corps of Engineers, Waterways Experiment Station, Vicksburg, MS:

Library

U.S. Bureau of Mines, Denver, CO;

P. L. Russell

U.S. Geological Survey:

W. Twenhofel, Denver, CO
W. Dudley, Denver, CO
Geologic Data Center, Mercury, NV (15)
K. W. King, Las Vegas, NV
Library, Denver, CO
Library, Menlo Park, CA

U.S. Geological Survey, Reston, VA:

Chief Hydrologist, WRD (Attn: Radiohydrology Section)
Library
Military Geology Unit
J. C. Reed, Jr.

GROUNDWATER POTENTIAL MODEL

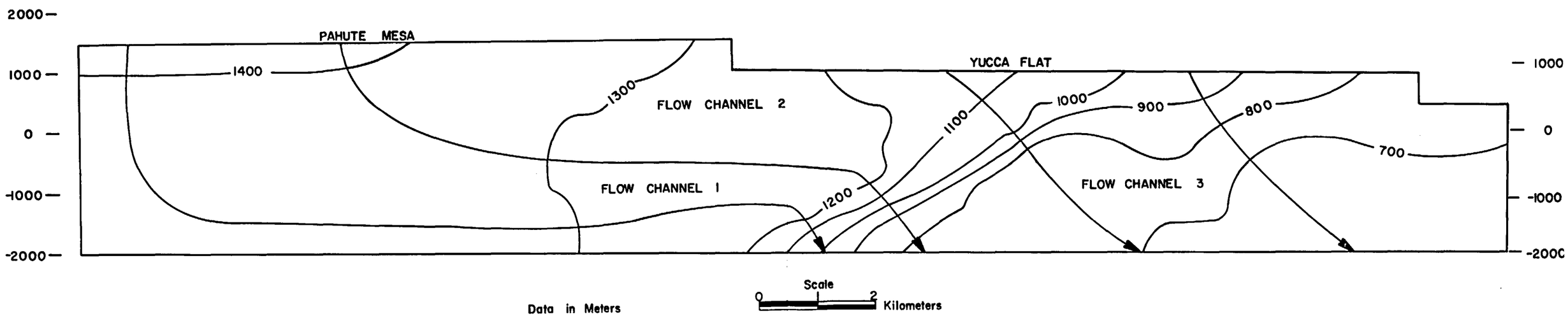

PLATE 2

GEOLOGIC CROSS SECTION FROM PAHUTE MESA TO YUCCA FLAT, NEVADA TEST SITE
COORDINATES N. 37° 11' 7" W. 116° 17' 40" TO N. 37° 9' 46" W. 116° 1' 47"

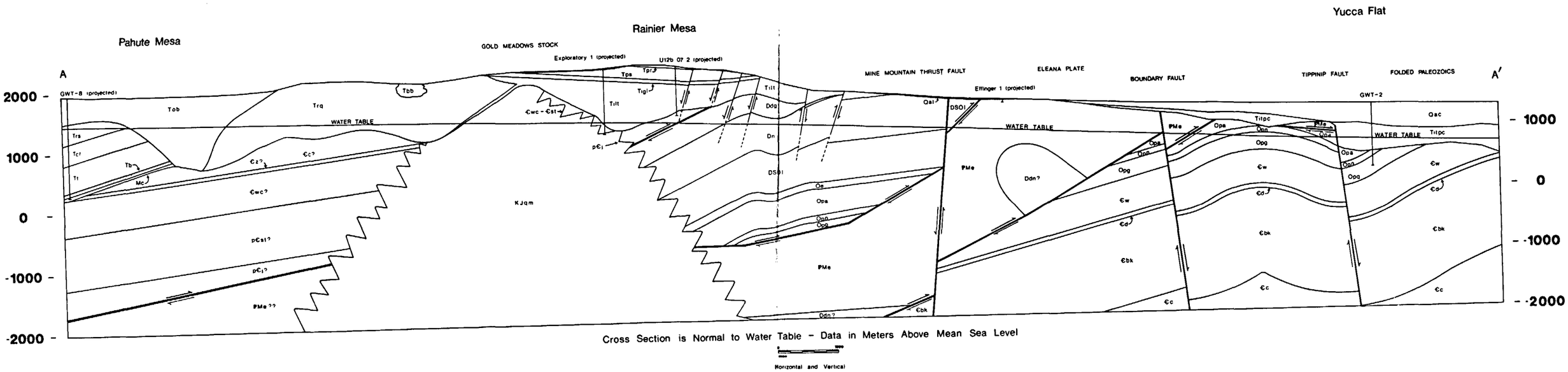

PLATE 1